

การพัฒนาระบบเคมีลูมิเนสเซนซ์สำหรับการตรวจวัดปริมาณรวมของสารต้านอนุมูลอิสระในไวน์  
และเครื่องดื่ม



บทคัดย่อและแฟ้มข้อมูลฉบับเต็มของวิทยานิพนธ์ตั้งแต่ปีการศึกษา 2554 ที่ให้บริการในคลังปัญญาจุฬาฯ (CUIR)  
เป็นแฟ้มข้อมูลของนิสิตเจ้าของวิทยานิพนธ์ ที่ส่งผ่านทางบัณฑิตวิทยาลัย

The abstract and full text of theses from the academic year 2011 in Chulalongkorn University Intellectual Repository (CUIR)  
are the thesis authors' files submitted through the University Graduate School.

วิทยานิพนธ์นี้เป็นส่วนหนึ่งของการศึกษาตามหลักสูตรปริญญาวิทยาศาสตรมหาบัณฑิต  
สาขาวิชาเคมี ภาควิชาเคมี  
คณะวิทยาศาสตร์ จุฬาลงกรณ์มหาวิทยาลัย  
ปีการศึกษา 2559  
ลิขสิทธิ์ของจุฬาลงกรณ์มหาวิทยาลัย

DEVELOPMENT OF CHEMILUMINESCENCE SYSTEM FOR DETERMINATION OF TOTAL  
ANTIOXIDANT CONTENT IN WINES AND BEVERAGES

Miss Masinee Saowadee



A Thesis Submitted in Partial Fulfillment of the Requirements  
for the Degree of Master of Science Program in Chemistry

Department of Chemistry

Faculty of Science

Chulalongkorn University

Academic Year 2016

Copyright of Chulalongkorn University



เมลินีย์ เสาวดี : การพัฒนาระบบเคมีลูมิเนสเซนซ์สำหรับการตรวจวัดปริมาณรวมของสารต้านอนุมูลอิสระในไวน์และเครื่องดื่ม (DEVELOPMENT OF CHEMILUMINESCENCE SYSTEM FOR DETERMINATION OF TOTAL ANTIOXIDANT CONTENT IN WINES AND BEVERAGES) อ.ที่ปรึกษาวิทยานิพนธ์หลัก: ดร.ภัสสรพล งามอุโฆษ, 63 หน้า.

งานวิจัยนี้ได้มีการพัฒนาระบบการตรวจวัดเคมีลูมิเนสเซนซ์ร่วมกับเทคนิคการวิเคราะห์แบบไหลสำหรับการตรวจวัดหาปริมาณรวมของสารต้านอนุมูลอิสระในตัวอย่างไวน์และเครื่องดื่ม เทคนิคนี้จะอาศัยปฏิกิริยาการเรืองแสงของลูมินอลและไฮโดรเจนเปอร์ออกไซด์ในสภาวะเบส โดยใช้โพแทสเซียมเพอร์ไซยาไนด์เป็นตัวเร่งปฏิกิริยา สารต้านอนุมูลอิสระที่มีอยู่ในตัวอย่างจะทำหน้าที่ยับยั้งสารอนุมูลอิสระ ทำให้การเกิดปฏิกิริยาเรืองแสงน้อยลง ซึ่งความเข้มแสงเคมีลูมิเนสเซนซ์ที่ปลดปล่อยออกมา มีความสัมพันธ์กับปริมาณของสารต้านอนุมูลอิสระที่มีอยู่ในตัวอย่าง งานวิจัยนี้ได้มีการออกแบบและสร้างระบบการตรวจวัดเคมีลูมิเนสเซนซ์และฟลูว์เซลล์ที่มีลักษณะเป็นขดรูปกันหอยซึ่งทำมาจากวัสดุที่มีราคาถูก เคมีลูมิเนสเซนซ์ฟลูว์เซลล์ทำมาจากวัสดุพอลิเมอร์ที่มีสีขาวขุ่น โพลีเมทิลเมทาไครเลต หรืออะคริลิกพลาสติก นอกจากนี้ยังมีการใช้อุปกรณ์ตรวจจับแสงที่มีขนาดเล็กและราคาถูก ทำให้สามารถพัฒนาเครื่องมือที่มีขนาดเล็กลงได้ ดังนั้นระบบการตรวจวัดเคมีลูมิเนสเซนซ์ที่พัฒนาขึ้นมาจึงมีราคาถูก ขนาดเล็ก สามารถพกพาได้ และยังสามารถนำไปใช้งานร่วมกับเทคนิคการวิเคราะห์แบบไหลได้อีกด้วย งานวิจัยนี้ได้ศึกษาสภาวะที่เหมาะสมสำหรับการตรวจวัดหาปริมาณรวมของสารต้านอนุมูลอิสระและพบว่าช่วงความเป็นเส้นตรงสำหรับกรดแกลลิกเท่ากับ 0.5 ถึง 5.0 มิลลิโมลาร์ ซึ่งมีขีดจำกัดต่ำสุดในการตรวจวัดเท่ากับ 0.25 มิลลิโมลาร์ และขีดจำกัดต่ำสุดในการวิเคราะห์เท่ากับ 0.84 มิลลิโมลาร์ สำหรับการศึกษาความสามารถในการทำซ้ำพบว่าค่าเปอร์เซ็นต์ความเบี่ยงเบนมาตรฐานสัมพัทธ์อยู่ในช่วง 2.2 ถึง 5.4 นอกจากนี้ยังมีการศึกษาความถูกต้องของวิธี ซึ่งจากผลการทดลองพบว่าค่าเปอร์เซ็นต์การได้กลับคืนมาอยู่ในช่วง 95.8 ถึง 105.6 และจำนวนตัวอย่างที่สามารถวัดได้ในหนึ่งชั่วโมงเท่ากับ 60 ตัวอย่าง สำหรับวิธีการวิเคราะห์ที่ได้พัฒนาขึ้นมานั้นสามารถนำไปประยุกต์ใช้สำหรับการตรวจวัดปริมาณรวมของสารอนุมูลอิสระในตัวอย่างไวน์และเครื่องดื่มได้ ซึ่งผลการวิเคราะห์มีความน่าเชื่อถือและมีค่าใกล้เคียงกับวิธีมาตรฐาน นอกจากนี้ระบบการตรวจวัดเคมีลูมิเนสเซนซ์ร่วมกับเทคนิคการวิเคราะห์แบบไหลที่ได้พัฒนาขึ้นมายังมีความง่าย สะดวก รวดเร็ว มีความถูกต้องแม่นยำ และใช้ปริมาณสารเคมีน้อย

ภาควิชา เคมี

ลายมือชื่อนิสิต .....

สาขาวิชา เคมี

ลายมือชื่อ อ.ที่ปรึกษาหลัก .....

ปีการศึกษา 2559

# # 5772110223 : MAJOR CHEMISTRY

KEYWORDS: CHEMILUMINESCENCE / TOTAL ANTIOXIDANT CONTENT / SEQUENTIAL INJECTION ANALYSIS / FLOW-CELL / OPTICAL SENSORS

MASINEE SAOWADEE: DEVELOPMENT OF CHEMILUMINESCENCE SYSTEM FOR DETERMINATION OF TOTAL ANTIOXIDANT CONTENT IN WINES AND BEVERAGES.  
ADVISOR: PASSAPOL NGAMUKOT, Ph.D., 63 pp.

A sequential injection analysis (SIA) with chemiluminescence (CL) detection system was developed for determination of total antioxidant content (TAC) in wines and beverages. The method is based on the CL reaction between luminol and hydrogen peroxide in alkaline conditions with the presence of a  $K_3Fe(CN)_6$  catalyst. Antioxidants in the sample scavenged a reactive oxygen species as hydrogen peroxide and the decrease in CL intensity was observed that related to the TAC in sample. A cost-effective CL detection system with a home-made spiral configuration flow-cell was designed and constructed by inexpensive materials. The spiral chemiluminescence flow-cell was made from an opaque white polymer of polymethyl methacrylate (PMMA) or acrylic plastic. Furthermore, a light-to-voltage optical sensor was used as a low-cost alternative detector which is small and was also used for the miniaturization of instrument. Thus, the developed CL detection system is cost-effective, portable and has the ability to connect with flow-based systems. The optimum conditions of SIA-CL method were studied and the linear range for gallic acid was obtained ranging from 0.5 to 5.0  $mmol L^{-1}$ , the limit of detection (LOD) was 0.25  $mmol L^{-1}$  and the limit of quantitation (LOQ) was 0.84  $mmol L^{-1}$ . The reproducibility of the method was investigated and the between day %relative standard deviation was in the range of 2.2 to 5.4%. The %recovery was between 95.8 and 105.6% and the sample throughput was 60 samples  $h^{-1}$ . The proposed method was successfully applied for the determination of TAC in wine and beverage samples and the results were not significantly different when compare with the reference method. Therefore, the developed SIA-CL method is simple, fast, accurate and consume less reagent.

Department: Chemistry

Student's Signature .....

Field of Study: Chemistry

Advisor's Signature .....

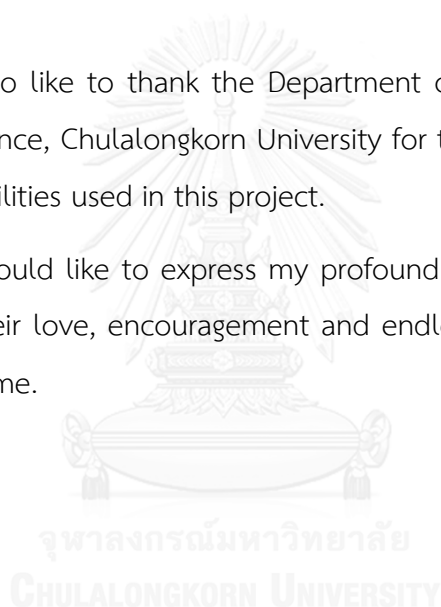
Academic Year: 2016

## ACKNOWLEDGEMENTS

I would like to express my gratitude to my advisor, Dr. Passapol Ngamukot for the encouragement, guidance and support throughout this project and during my Master's degree at Chulalongkorn University. Also, a special thanks to my thesis committee members, Assoc. Prof. Dr. Vudhichai Parasuk, Dr. Janjira Panchompoo and Dr. Phansak lamraksa for their input in suggestions. In addition, I would like to extend my special thank to Dr. Sira Nitiyanontakit for his advice and assistance.

I would also like to thank the Department of Chemistry and Machinery Unit, Faculty of science, Chulalongkorn University for their support in providing all equipments and facilities used in this project.

Finally, I would like to express my profound gratitude to my family and close friends for their love, encouragement and endless patience. Thank you for always believing in me.



## CONTENTS

	Page
THAI ABSTRACT .....	iv
ENGLISH ABSTRACT .....	v
ACKNOWLEDGEMENTS .....	vi
CONTENTS .....	vii
LIST OF TABLES .....	x
LIST OF FIGURES .....	xi
LIST OF ABBREVIATIONS .....	xiv
CHAPTER I INTRODUCTION.....	1
1.1 Introduction .....	1
1.2 Objectives of the research.....	3
CHAPTER II THEORY AND LITERATURE REVIEWS .....	4
2.1 Antioxidants in beverages .....	4
2.2 Chemiluminescence.....	6
2.2.1 Principle of chemiluminescence.....	6
2.2.2 Types of chemiluminescence.....	7
2.2.3 Basic instrumentation of chemiluminescence .....	8
2.2.4 Luminol-based chemiluminescence .....	9
2.3 Flow-based techniques .....	9
2.4 Literature reviews .....	11
CHAPTER III EXPERIMENTAL.....	14
3.1 Chemicals .....	14
3.2 Sample preparation.....	15

3.3 Chemiluminescence detector.....	15
3.2.1 Design and fabrication of chemiluminescence flow-cell.....	15
3.2.2 Development of chemiluminescence detector.....	17
3.4 Sequential injection analysis (SIA).....	18
3.4.1 Instrumentation.....	18
3.4.2 Experimental procedure for SIA-CL method.....	19
3.5 DPPH free radical scavenging method.....	20
3.6 Analytical performance.....	21
3.6.1 Linearity, LOD and LOQ.....	21
3.6.2 Precision.....	22
3.6.3 Trueness.....	22
3.7 Interference study.....	23
3.8 Real sample analysis.....	23
CHAPTER IV RESULTS AND DISCUSSION.....	24
4.1 Chemiluminescence characteristics.....	24
4.2 Optimization of SIA-CL system.....	25
4.2.1 Sequence of injection.....	25
4.2.2 Effect of sodium hydroxide concentration.....	26
4.2.3 Effect of luminol concentration.....	27
4.2.4 Effect of hydrogen peroxide concentration.....	28
4.2.5 Effect of potassium ferricyanide concentration.....	29
4.2.6 The volume of hydrogen peroxide.....	30
4.2.7 The volume of potassium ferricyanide.....	31



	Page
4.2.8 The volume of sample and standard solution .....	33
4.2.9 The volume of luminol.....	34
4.2.10 Effect of detection flow rate.....	35
4.2.11 Summary of the optimum conditions for the SIA-CL method .....	37
4.3 Analytical performance .....	38
4.3.1 Linearity, LOD and LOQ.....	38
4.3.2 Precision .....	40
4.3.3 Trueness .....	41
4.4 Interference study .....	42
4.5 Real sample analysis.....	43
CHAPTER V CONCLUSIONS.....	46
REFERENCES .....	47
APPENDIX A Chemiluminescence characteristics of luminol.....	54
APPENDIX B SIA-grams of gallic acid standard .....	55
APPENDIX C DPPH free radical scavenging method .....	56
APPENDIX D Correlation between SIA-CL method and DPPH method .....	57
APPENDIX E Development of chemiluminescence detector .....	58
VITA.....	63

## LIST OF TABLES

		Page
<b>Table 3.1</b>	List of wine and tea samples. ....	15
<b>Table 3.2</b>	Experimental sequence for SIA-CL method (SP: syringe pump, SV: selection valve). ....	20
<b>Table 4.1</b>	The optimum conditions for the SIA-CL method (S: sample, O: oxidant or H <sub>2</sub> O <sub>2</sub> , L: luminol, C: catalyst or K <sub>3</sub> Fe(CN) <sub>6</sub> ). ....	37
<b>Table 4.2</b>	The within-day repeatability and between-days reproducibility of the SIA-CL method.....	40
<b>Table 4.3</b>	Recovery study of gallic acid in wine and tea samples.....	41
<b>Table 4.4</b>	The acceptable concentration of interfering compounds in the determination of gallic acid by SIA-CL method.....	42
<b>Table 4.5</b>	Total antioxidant content in wine and tea samples obtained by the SIA-CL and DPPH method. ....	43
<b>Table 4.6</b>	The GAE values of wine and tea samples obtained by the proposed method and published literature. ....	44

## LIST OF FIGURES

	Page
<b>Figure 2.1</b>	Chemical structures of synthetic antioxidants..... 4
<b>Figure 2.2</b>	Chemical structures of natural antioxidants found in plant-derived beverages..... 5
<b>Figure 2.3</b>	Jablonski diagram illustrating energy level and transition. F: fluorescence, C: chemiluminescence, P: phosphorescence, CD: collisional deactivation, IC: internal conversion, ISC: intersystem crossing, $S_0$ : ground singlet state, $S_1$ and $S_2$ : excited singlet state and $T_1$ : excited triplet state. .... 6
<b>Figure 2.4</b>	Types of chemiluminescence reactions. A: substrate, B: oxidant, C and D: products, F: fluorophore..... 7
<b>Figure 2.5</b>	Schematic diagram of a basic chemiluminescence system..... 8
<b>Figure 2.6</b>	The oxidation of luminol in the presence of hydrogen peroxide and catalyst..... 9
<b>Figure 2.7</b>	Schematic diagram of flow injection analysis. .... 10
<b>Figure 2.8</b>	Schematic diagram of sequential injection analysis. .... 10
<b>Figure 3.1</b>	The 3D model of chemiluminescence flow-cell..... 16
<b>Figure 3.2</b>	The top face (solid view), bottom face (transparent view) and side view of flow-cell. .... 16
<b>Figure 3.3</b>	Chemiluminescence flow-cell with a spiral channel configuration. .... 17
<b>Figure 3.4</b>	Development of chemiluminescence detector. .... 18

<b>Figure 3.5</b>	Schematic diagram of SIA system. SP: syringe pump, HC: holding coil, SV: selection valve, RC: reaction coil, FC: flow-cell, PC: personal computer.....	19
<b>Figure 4.1</b>	Chemiluminescence from the reaction of luminol with $H_2O_2$ and $K_3Fe(CN)_6$ in a spiral flow-cell.....	24
<b>Figure 4.2</b>	The effect of aspiration sequence on CL intensity. S: sample (blank), C: catalyst ( $K_3Fe(CN)_6$ ), O: oxidant ( $H_2O_2$ ) and L: luminol.....	25
<b>Figure 4.3</b>	The effect of sodium hydroxide concentration on CL intensity...	26
<b>Figure 4.4</b>	The effect of luminol concentration on CL intensity.....	27
<b>Figure 4.5</b>	The effect of hydrogen peroxide concentration on CL intensity. ....	28
<b>Figure 4.6</b>	The effect of potassium ferricyanide concentration on CL intensity. ....	29
<b>Figure 4.7</b>	SIA-grams recorded from various volumes of hydrogen peroxide.....	30
<b>Figure 4.8</b>	The effect of hydrogen peroxide volume on CL intensity.....	31
<b>Figure 4.9</b>	SIA-grams recorded from various volumes of potassium ferricyanide.....	32
<b>Figure 4.10</b>	The effect of potassium ferricyanide volume on CL intensity. ....	32
<b>Figure 4.11</b>	SIA-grams recorded from various volumes of gallic acid.....	33
<b>Figure 4.12</b>	The effect of gallic acid volume on signal suppression. ....	34
<b>Figure 4.13</b>	The effect of luminol volume on CL intensity: (A) 1000 $\mu L$ of luminol, (B) 1500 $\mu L$ of luminol, (C) 2000 $\mu L$ of luminol, (D) 2500 $\mu L$ of luminol.....	35
<b>Figure 4.14</b>	The effect of detection flow rate on CL intensity. ....	36

<b>Figure 4.15</b>	SIA-grams of blank solution ( $I_0$ ) and antioxidant solution ( $I_s$ ), $C_{\text{gallic acid}} = 4.0 \text{ mmol L}^{-1}$ ..... 38
<b>Figure 4.16</b>	A calibration curve of gallic acid using SIA-CL method..... 39
<b>Figure 4.17</b>	Paired t-test comparison of % antioxidant activity between SIA-CL method and DPPH method..... 45
<b>Figure A1</b>	Chemiluminescence spectrum of luminol with hydrogen peroxide with the presence of potassium ferricyanide catalyst recorded by AvaSpec-2048 fiber-optic spectrophotometer. .... 54
<b>Figure B1</b>	SIA-grams of various gallic acid concentrations using SIA-CL method..... 55
<b>Figure C1</b>	A calibration curve of gallic acid using DPPH method..... 56
<b>Figure D1</b>	Correlation plot between the SIA-CL method and DPPH method for wine samples (n=3). .... 57
<b>Figure D2</b>	Correlation plot between the SIA-CL method and DPPH method for tea samples (n=3). .... 57
<b>Figure E1</b>	The 3D design of developed chemiluminescence detector. .... 58

## LIST OF ABBREVIATIONS

ABTS	2,2'-azinobis (3-ethylbenzothiazolline-6-sulfonic acid)
CL	chemiluminescence
DAQ	data acquisition
DPPH	2,2-diphenyl-1-picrylhydrazyl
EDTA	ethylenediaminetetraacetic acid
FEP	fluorinated ethylene propylene
FIA	flow injection analysis
FRAP	ferric reducing antioxidant power
g	gram
GAE	gallic acid equivalent
HPLC	high performance liquid chromatography
HRP	horseradish peroxidase
i.d.	internal diameter
L	liter
$\mu\text{L}$	microliter
LOD	limit of detection
LOQ	limit of quantitation
MSFIA	multisyringe flow injection analysis
M	molar or mole per liter
min	minute
mL	milliliter

mm	millimeter
mmol	millimole
nm	nanometer
ORAC	oxygen radical absorbance capacity
PDA	photodiode array
PMMA	polymethyl methacrylate
PMT	photomultiplier tube
PTFE	polytetrafluoroethylene
$R^2$	correlation coefficient
RSD	relative standard deviation
SD	standard deviation
SIA	sequential injection analysis
TAC	total antioxidant content or total antioxidant capacity
TEAC	trolox equivalent antioxidant capacity

# CHAPTER I

## INTRODUCTION

### 1.1 Introduction

Antioxidants are molecules that prevent cell damage caused by free radicals. Antioxidants are found mostly in plant-derived food and beverages such as salad, fresh fruits, herbs, species, wine, tea and juices [1]. The consumption of antioxidant-rich foods is beneficial to human health. There are many research shows that antioxidant compounds can prevent several disorders such as diabetes, cancer and cardiovascular diseases [2-5]. Thus, the determination of total antioxidant content (TAC) in food products is necessary for the consumers and quality control in the food and beverage industry.

Analytical techniques commonly used for the determination of TAC in food and beverage samples are spectrophotometry (e.g. antioxidant activity assay by FRAP, TEAC, ABTS, DPPH and ORAC method [6-9]), chromatography (e.g. evaluation of antioxidant activity by on-line HPLC-DPPH assay [10] and HPLC-PDA method [11]) and electrochemistry (e.g. determination of total antioxidant capacity by electrochemical biosensor [12, 13] and cyclic voltammetry [14]). The methods most often used for determination of TAC are spectrophotometry. However, the disadvantages of these methods are low sensitivity and selectivity, long reaction time and low accuracy due to interferences caused by colored compounds in the sample [15]. Therefore, the development of a simple, rapid and more reliable method for the TAC determination in food samples is needed.

Chemiluminescence (CL) methods have been widely used for the determination of TAC because these methods offer many advantages such as high sensitivity, selectivity and wide linear dynamic range [16]. In addition, the apparatus of CL detection system is simpler and less expensive (because no external light source is needed) than spectrophotometric methods. Recently, the CL detection



system was combined with flow-based techniques such as flow injection analysis (FIA) and sequential injection analysis (SIA). These on-line systems can be fully automated and consume less chemical reagent. Consequently, the combination of these two techniques can be used to reduce analysis time and improve the precision of measurements [17].

Several CL reagents are used in the assessment of antioxidant activity such as luminol [18-23], lucigenin [24], potassium permanganate [25, 26], peroxyoxalate [27, 28] and tris(2,2'- bipyridine) ruthenium(II) or  $[\text{Ru}(\text{bpy})_3]^{2+}$  [29]. The most widely used CL reagent is luminol because of its well-known characteristic, fast reaction time and does not require mixing in an organic solvent. For luminol-based chemiluminescence, the most effective oxidant under basic conditions is hydrogen peroxide and the reaction can be catalyzed by transition metals (e.g. Co(II), Cr(II), Cu(II), Fe(II) and Fe(III)) and their complexed forms (e.g. ferrocene ( $\text{Fe}(\text{C}_5\text{H}_5)_2$ ) and ferricyanide ( $[\text{Fe}(\text{CN})_6]^{3-}$ )) [30].

In this work, the sequential injection analysis with chemiluminescence (SIA-CL) method was developed for the determination of TAC in plant-derived beverage samples. The method is based on the inhibition of luminol chemiluminescence by antioxidants in the sample as it scavenged a portion of the oxidant resulting in a decrease in CL intensity. A cost-effective chemiluminescence detection system was fabricated and applied to the flow-based techniques. The proposed method was validated in terms of linearity, selectivity, detection limit, accuracy and precision (repeatability and reproducibility). Moreover, the TAC measurement in beverage samples obtained from the developed SIA-CL method was compared to the DPPH method.

## 1.2 Objectives of the research

1. To develop the SIA-CL method for the determination of total antioxidant capacity.
2. To develop an inexpensive and portable instrument for chemiluminescence detection.
3. To apply the proposed method for the determination of total antioxidant capacity in wine and beverage samples.



## CHAPTER II

### THEORY AND LITERATURE REVIEWS

#### 2.1 Antioxidants in beverages

Antioxidants play an important role in the protection of cell damage caused by free radicals. Based on their activity, antioxidants can be divided into two classes: primary or natural antioxidant (e.g. vitamins (A, C and E),  $\beta$ -carotenoid and phenolic compounds) and secondary or synthetic antioxidants (e.g. butylated hydroxytoluene (BHT), butylated hydroxyanisole (BHA), tertiary butylhydroquinone (TBHQ) and propyl gallate) [31]. Antioxidants are found in beverages such as wine, beer, tea, coffee, fruit juices, herbal infusion drinks and other soft drinks. In food and beverage industry, synthetic antioxidants are added to preserve the product and extend shelf life. However, natural antioxidants are safer, more efficient and potent than synthetic antioxidants [32]. The most antioxidants found in plant-derived beverages are phenolic or polyphenol compounds which exhibit strong antioxidant activity both *in vivo* and *in vitro* studies [1]. Some examples of natural antioxidants and synthetic antioxidants are shown in Figure 2.1 and 2.2.

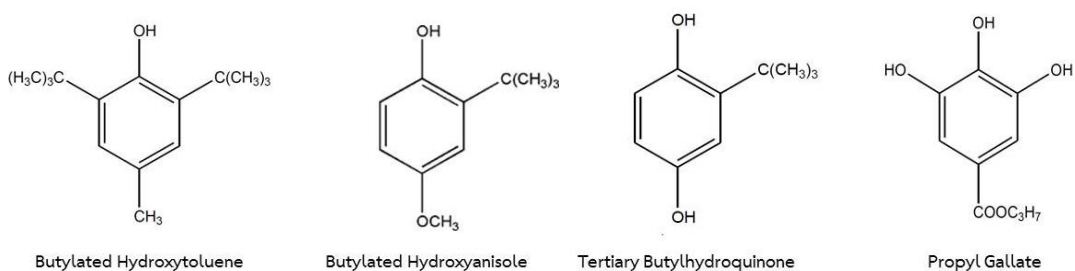


Figure 2.1 Chemical structures of synthetic antioxidants.



## 2.2 Chemiluminescence

### 2.2.1 Principle of chemiluminescence

Chemiluminescence is a phenomenon of the emission of light in the visible or near-infrared region as a result of a chemical reaction. In chemiluminescence, the reactions produce the unstable products in an electronically excited state, which then return to ground state by a release of energy in the form of light. The process of light emission in chemiluminescence and photoluminescence (fluorescence and phosphorescence) is the same. However, the excitation process in photoluminescence occurs by the absorption of light in the ultraviolet or visible region as can be seen in Figure 2.3.

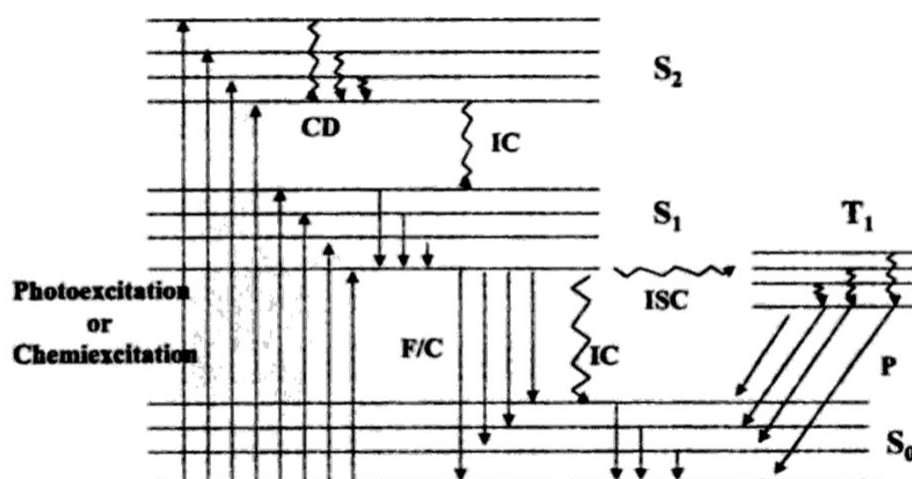


**Figure 2.3** Jablonski diagram illustrating energy level and transition. F: fluorescence, C: chemiluminescence, P: phosphorescence, CD: collisional deactivation, IC: internal conversion, ISC: intersystem crossing,  $S_0$ : ground singlet state,  $S_1$  and  $S_2$ : excited singlet state and  $T_1$ : excited triplet state.

## 2.2.2 Types of chemiluminescence

The two main types of chemiluminescence mechanisms are illustrated in Figure 2.4. In direct CL reaction, two compounds A and B, usually a chemiluminescent precursor and oxidant, react to form a product  $C^*$  in an excited state which then decays to ground state accompanied by photon or light emission. In case of indirect CL reaction, the chemical energy of product  $C^*$  in an excited state is transferred to a fluorophore (F) and after excitation is relaxed to ground state along with photon emission. This process can be used for those molecules that are not able to be directly generated in CL reactions [16].

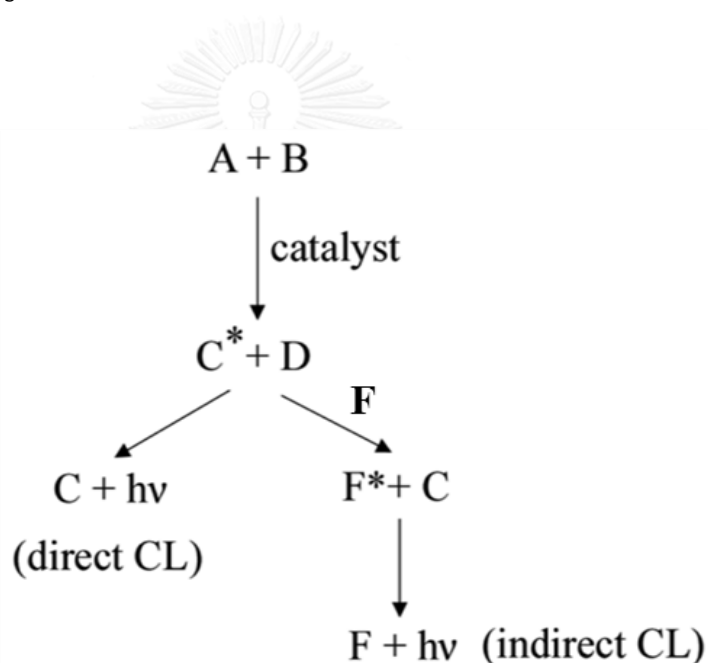


**Figure 2.4** Types of chemiluminescence reactions. A: substrate, B: oxidant, C and D: products, F: fluorophore.

### 2.2.3 Basic instrumentation of chemiluminescence

The chemiluminescence detection system (Figure 2.5) consists of a light-tight housing, reaction cell, sample and reagent introduction device, light detector and data acquisition system. In the housing, the reaction cell (e.g. flow-cell, test tube and microplate) is positioned close to detector to improve the detection efficiency and the chamber must be sealed from external or ambient light to reduce interferences. Moreover, lenses and mirror can be used for focusing and reflection of the light on to the detector. Several systems commonly used for sample and reagent introduction are static systems (batch or discrete sampling instrument) and flowing stream (continuous-flow or stopped-flow system). In the flow system, the sample containing the analyte is injected to a carrier stream and delivered to the detection zone of reaction cell. The advantages of this system are rapid, less sample and reagent consumption. For the CL flow-cell, the most often used cell design is a long spiral configuration, made from any materials such as quartz, glass, acrylic and other plastics. Mostly, photomultiplier tubes (PMT) are used in CL detection system because of its high sensitivity, low noise and suitable for low light detection. However, they are more expensive than photodiodes [16].

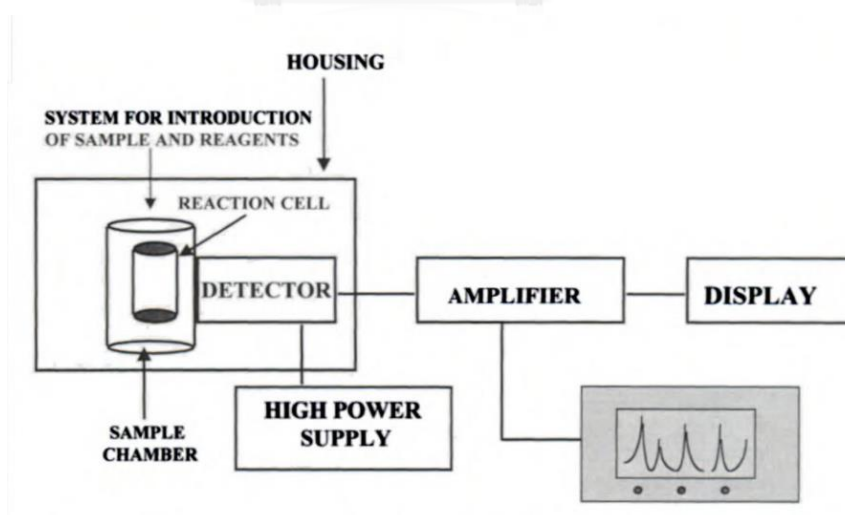
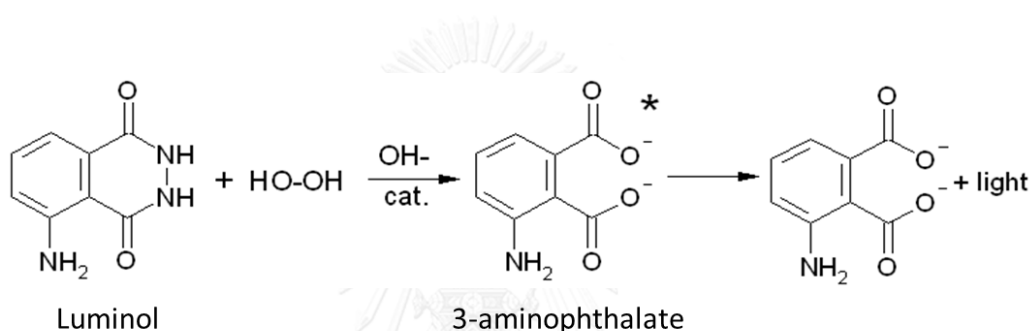


Figure 2.5 Schematic diagram of a basic chemiluminescence system.

### 2.2.4 Luminol-based chemiluminescence

Luminol or 3-aminophthalhydrazide is the most widely used chemiluminescent agent. It is well-known, has a fast reaction time and does not require mixing in an organic solvent. The most effective oxidant for luminol-based chemiluminescence is hydrogen peroxide. The oxidation of luminol by an oxidant in basic solution in the presence of catalyst (e.g.  $[\text{Fe}(\text{CN})_6]^{3-}$ ,  $\text{Co}(\text{II})$  and  $\text{Cu}(\text{II})$ ) formed the intermediate species of 3-aminophthalate dianion that is excited and return to ground state with blue light emission (Figure 2.6) [33].



**Figure 2.6** The oxidation of luminol in the presence of hydrogen peroxide and catalyst.

### 2.3 Flow-based techniques

Flow-based analysis is based on the continuous flow of solution or carrier steam and the injection of sample into carrier steam. The most common flow-based analysis techniques are flow injection analysis (FIA) and sequential injection analysis (SIA). In the FIA process, the small volume of sample solution is injected into a carrier steam containing reagents to produce the reaction at a reaction coil and the result of the reaction is monitored by the detector [34]. Schematic diagram of flow injection analysis is presented in Figure 2.7.

A sequential injection analysis (SIA) is the second generation of the flow injection analysis. The SIA system consists of a syringe pump, holding coil, selection valve and detector. Schematic diagram of sequential injection analysis is shown in



Figure 2.8. In the SIA process, a portion of sample and reagents are sequentially aspirated into a holding or mixing coil. Then, the product produced from the reaction is dispensed to the detector. All processes of SIA are controlled by the program on computer. The SIA technique can be classified as discontinuous flow process that require less consumption of reagents than FIA technique [35].

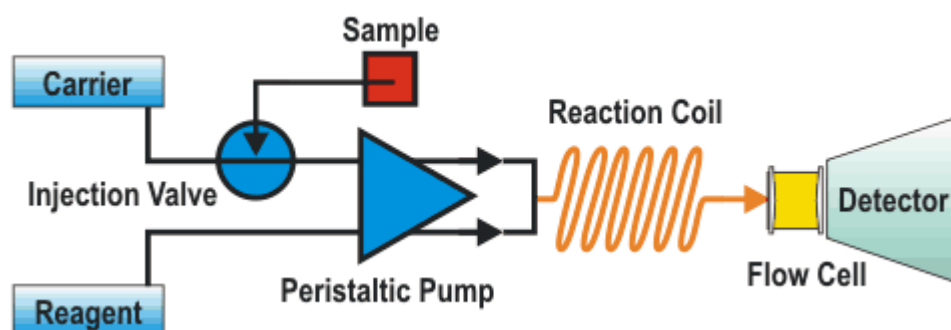


Figure 2.7 Schematic diagram of flow injection analysis.

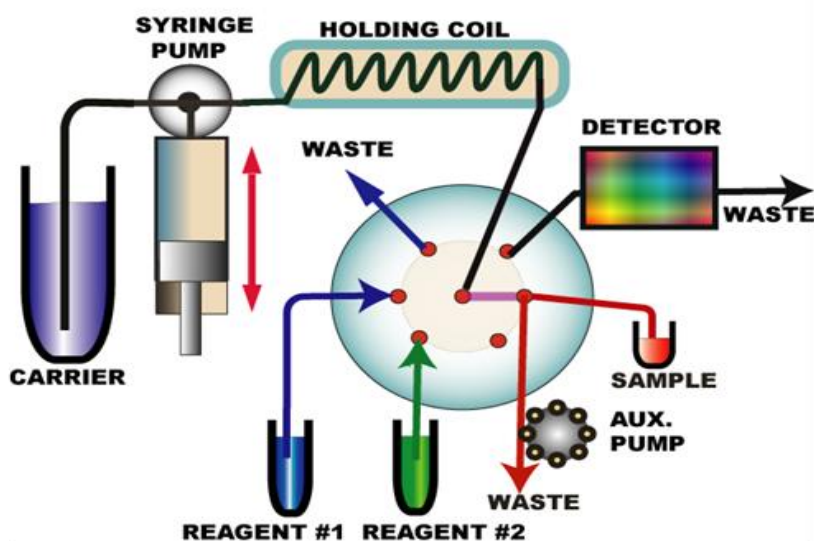


Figure 2.8 Schematic diagram of sequential injection analysis.

## 2.4 Literature reviews

There are many reports of flow-based analysis coupled with CL detection for the determination of TAC and total phenolic compounds in food samples. Murillo Pulgarín et al. [36] reported a flow injection analysis (FIA) for the determination of the TAC in teas, wines and grape seeds. The method is based on the attenuation of luminol-Co(II)-EDTA-perborate chemiluminescence by the antioxidants in the samples. The results showed that the use of Co(II)-EDTA complex, which acted as a catalyst, resulting in a constant and reproducible CL emission. The proposed method is simple and fast, requiring less than 5 min per one of sample (12 samples h<sup>-1</sup>). Additionally, this method consumes less chemical reagent and does not require extra procedure for sample pretreatment. Therefore, the proposed method is considered as an economical and environmentally friendly method for the determination of TAC in food samples.

Araujo et al. [37] presented a multisyringe flow injection analysis (MSFIA) and sequential injection analysis (SIA) techniques for the screening of phenolic compound in food and environmental samples. The developed SIA-MSFIA was connected with CL detection system, which is based on the CL reaction of luminol-hydrogen peroxide-horseradish peroxidase (HRP). It was found that polyphenol such as gallic acid and tannic acid act as inhibitors for the CL system. The linear range of tannic acid was 0.01-5 mg L<sup>-1</sup> and the time required for a complete analysis cycle was 400 s (9 samples h<sup>-1</sup>). In conclusion, the SIA-MSFIA-CL method provides a good efficiency when compared to the batch reference methods.

Fassoula et al. [18] reported a sequential injection analysis (SIA) techniques with CL detection for the rapid determination of the TAC in wine samples. The method is based on the oxidation of luminol in alkaline medium using hydrogen peroxide with the presence of Co(II) catalyst. In this work, gallic acid was used as a standard antioxidant because it is a main phenolic component of wines. The effect of catalyst was studied and the results shown that in the absence of catalyst, the CL signal was weak and poor sensitivity and linear range were observed. The linearity of gallic acid was in the range of  $1.0 \times 10^{-6}$  to  $2.0 \times 10^{-4}$  mol L<sup>-1</sup>, the recovery was 96.7

to 97.3% and the sampling frequency was 60 samples  $\text{h}^{-1}$ . The developed SIA-CL method was compared to the DPPH free radical scavenging method and Folin-Ciocalteu (FC) method. It was found that the present method could be used for ranking samples according to their TAC with respect to the standard DPPH method.

Karamelas et al. [20] developed a novel hybrid flow injection and sequential injection (FIA-SIA) method coupled with CL detection for the assessment of the TAC in wine samples. This method is based on the oxidation of luminol using potassium permanganate in alkaline solution. The antioxidants in sample scavenged an oxidant such as potassium permanganate causing a decrease in CL signal. The concentration range of gallic acid was  $0.90 \mu\text{mol L}^{-1}$  to  $15 \mu\text{mol L}^{-1}$  and the % recoveries were 93 and 96%. In this work, the proposed FIA-SIA configuration combines the advantages from both FIA and SIA. Therefore, the FIA-SIA-CL method is faster, simpler and lower in reagent consumption than the conventional flow-based analysis method. Furthermore, the method is fully automated, accurate and robust.

For the catalyst used in luminol-based chemiluminescence, Jain [38] studied the effect of catalyst on luminol-hydrogen peroxide CL reaction in aqueous medium. It was found that the CL behavior depends on the catalyst used and the suggested transition metal catalysts for use in this reaction are Cu, Fe, Co, Cr and Mn. The best catalyst on luminol-hydrogen peroxide CL reaction in aqueous medium is  $\text{CuSO}_4 \cdot 5\text{H}_2\text{O}$ . Moreover, Alapont et al. [39] reported a ferricyanide or hexacyanoferrate (III),  $[\text{Fe}(\text{CN})_6]^{3-}$  is an oxidant with a constant redox potential between pH 4 and 13. On the other hand, this species can act as a catalyst and co-oxidant on the luminol-hydrogen peroxide CL reaction in alkaline condition.

For the CL flow-cell, Mohr et al. [40] and Terry et al. [41] proposed a new design of flow-cells for CL detection system. It was found that the intensity of light transferred to the detector from the opaque white chip polymer (sealed with transparent film) is higher than the transparent chip and coiled-tubing flow-cell because the opacity of the materials reduces the loss of light through the surface and therefore increases the CL intensity.

Previous researches showed that there has been some problem with high cost and complexity of the instrument. Therefore, the development of a cost-effective CL detection system and simple configuration of flow-based analysis is needed.



## CHAPTER III

### EXPERIMENTAL

#### 3.1 Chemicals

Gallic acid, 2,2-diphenyl-1-picrylhydrazyl (DPPH), luminol (97%), sucrose and fructose were purchased from Sigma-Aldrich, Germany. Glucose and potassium ferricyanide ( $K_3Fe(CN)_6$ ) were supplied by Carlo erba, France. Sodium hydroxide, ethanol and 30% hydrogen peroxide ( $H_2O_2$ ) were obtained from Merck, Germany. All chemicals used in this work were of analytical grade and were used without further purification.

The  $3.0 \times 10^{-3} \text{ mol L}^{-1}$  solution of  $H_2O_2$  was freshly prepared by diluting 0.938 mL of 30%  $H_2O_2$  in 25 mL of deionized water.

The  $0.3 \text{ mol L}^{-1}$  solution of NaOH was prepared by dissolving 6.0 g of NaOH in deionized water and made volume up to 500 mL.

Luminol solution ( $4.0 \times 10^{-3} \text{ mol L}^{-1}$ ) was prepared by dissolving 0.1772 g of luminol in  $0.3 \text{ mol L}^{-1}$  of NaOH solution and adjusting volume up to 250 mL with  $0.3 \text{ mol L}^{-1}$  NaOH solution. The luminol solution was stored in the dark and cool place.

Stock solution of  $1.0 \times 10^{-2} \text{ mol L}^{-1}$  gallic acid was prepared daily by dissolving 0.0425 g of the solid compound in 25 mL of deionized water.

The solution of  $0.2 \text{ mol L}^{-1}$  potassium ferricyanide was prepared by dissolving 1.6462 g of potassium ferricyanide in 25 mL of deionized water.

The  $6.0 \times 10^{-5} \text{ mol L}^{-1}$  solution of DPPH was freshly prepared by dissolving 0.0059 g of the solid compound in 250 mL of ethanol and kept in the dark.

### 3.2 Sample preparation

Different types of wine and ready to drink tea samples were purchased from local supermarkets and listed in Table 3.1. For the SIA-CL method, the samples were diluted with deionized water (red wine was diluted 10-fold; white and rose wine were diluted 2-fold; green and oolong tea were diluted 2-fold; black tea was used without dilution). For the DPPH method, the samples were diluted with deionized water (red wine was diluted 20-fold; white and rose wine were diluted 5-fold; green and oolong tea were diluted 10-fold; black tea was diluted 2-fold).

**Table 3.1** List of wine and tea samples.

No. of sample	Type of sample	Location
<b>Wine samples</b>		
1	red wine (shiraz)	
2	white wine (Chardonnay)	South Africa
3	rose wine (Cabernet Sauvignon)	
<b>Tea samples</b>		
4	green tea	
5	oolong tea	Thailand
6	black tea	

### 3.3 Chemiluminescence detector

#### 3.2.1 Design and fabrication of chemiluminescence flow-cell

The flow-cell was designed by SolidWorks 2012 software (SolidWorks Corp., USA) and the model was converted into machine code using Cut2D software (Vectric Ltd., UK). The 3D model of flow-cell was shown in Figure 3.1 and 3.2. The

flow-cell had dimension of 45 mm × 60 mm × 12 mm and the top face contained a 30 mm diameter of a spiral-configuration reaction zone. There are two ports for solution inlet and outlet which had a diameter of 5 mm.

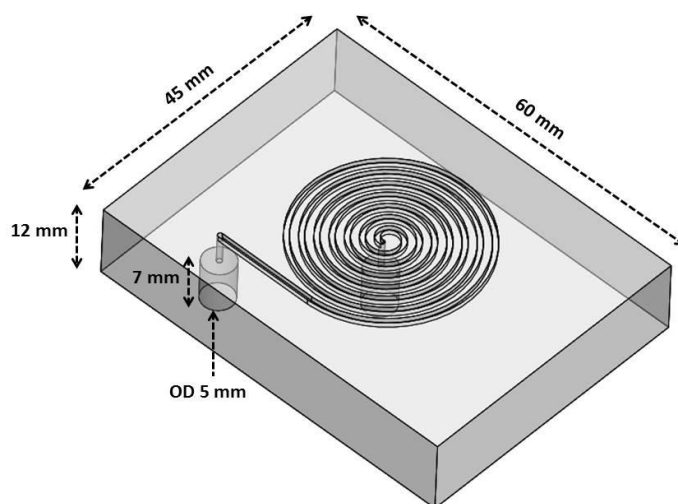


**Figure 3.1** The 3D model of chemiluminescence flow-cell.

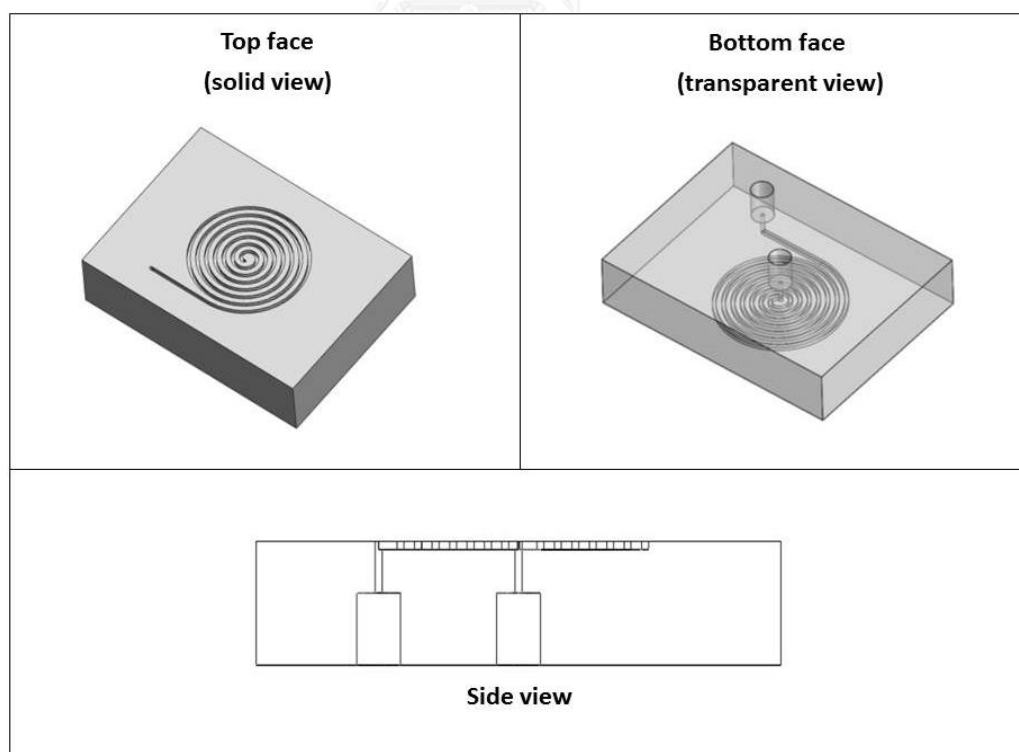


**Figure 3.2** The top face (solid view), bottom face (transparent view) and side view of flow-cell.

The chemiluminescence flow-cell with a spiral configuration (Figure 3.3) was fabricated from a white polymer sheet of polymethyl methacrylate (PMMA) or acrylic plastic (12 mm thick sheets). The channel (1 mm × 1 mm) was milled with a ball nose end mill (R0.5 mm) using CNC milling machine (Spar Mechatronics Co.,Ltd, Thailand). The channel length was 385 mm and total volume of detection zone was 347  $\mu$ L. The universal optical sealing tape (Bio-red Laboratories Inc., USA) was used to seal the channel. The tape was cut to size and then applied to the flow-cell surface. Solution lines were connected to the flow-cell using 1/4-28 super flangeless fittings (IDEX Health & Science, USA).



**Figure 3.3** Chemiluminescence flow-cell with a spiral channel configuration.

### 3.2.2 Development of chemiluminescence detector

The developed chemiluminescence detector (Figure 3.4) consisted of a home-made spiral flow-cell where the chemiluminescence reaction will occur, two lenses from illuminated loupe (40X, 25 mm diameter) for focusing the light to the optical sensor, a light-to-voltage optical sensor (TSL12S, Texas Advanced Optoelectronic Solutions Inc., USA) was used to collect the emitted light from the chemiluminescence reaction and a power supply (YwRobot Corp., China) was used to stabilize and supply voltage to the sensor. The output signal was recorded using a



data acquisition (DAQ) device (National Instruments, Austin, TX) with LabVIEW software. The total dimension of the chemiluminescence detector was 116 mm × 192 mm × 90 mm. The black box was constructed from black acrylic plastic (3 mm thick sheets).

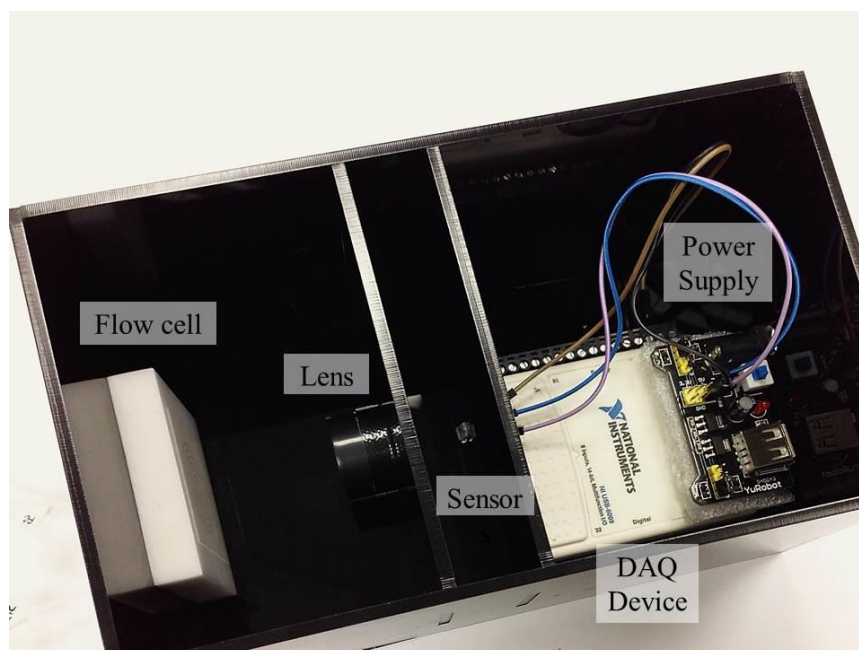
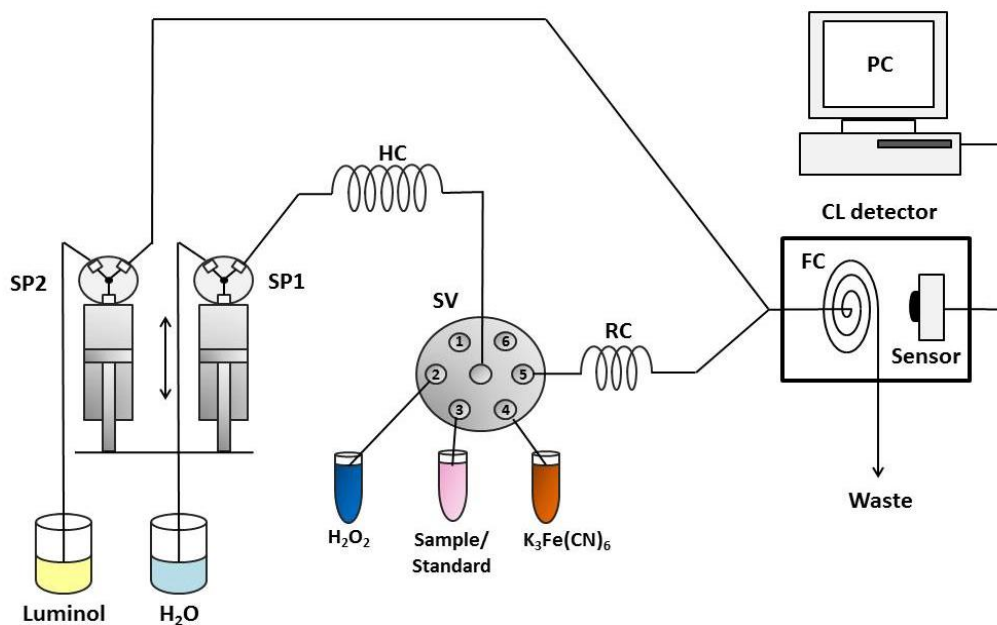


Figure 3.4 Development of chemiluminescence detector.

### 3.4 Sequential injection analysis (SIA)

#### 3.4.1 Instrumentation

A schematic diagram of the sequential injection analysis (SIA) system for the determination of total antioxidant content in beverage samples is shown in Figure 3.5. Two syringe pumps (Chemyx Inc., USA) and a six-port selection valve (IDEX Health & Science, USA) were used to control flow rate of carrier and reagents. The reaction coil was set separately from a holding coil to increase the mixing of the reagent solutions. A home-made CL detector consisted of a spiral flow-cell and optical sensor. The pump tubing used was PTFE 1.5 mm i.d. (Grace, USA) and all the others tubing were FEP 0.75 mm i.d. (IDEX Health & Science, USA).



**Figure 3.5** Schematic diagram of SIA system. SP: syringe pump, HC: holding coil, SV: selection valve, RC: reaction coil, FC: flow-cell, PC: personal computer.

### 3.4.2 Experimental procedure for SIA-CL method

For the system preparation process, all the solutions lines were filled with the appropriate reagents. The experimental sequence for SIA-CL is shown in Table 3.1. A deionized water and luminol were aspirated into the syringe which was set separately. Then, a zone of hydrogen peroxide, sample or standard and  $K_3Fe(CN)_6$  were aspirated to the holding coil. The stacked zone of sample and reagents were dispensed to mix with luminol and delivered to the flow-cell. The CL signal was then measured by the optical sensor. The mean of signal was calculated from five measurements for each sample. The calibration graph was plotted between the concentration of gallic acid and signal suppression. The signal suppression due to the antioxidant activity ( $\Delta I\%$ ) was calculated according to the formula:

$$\Delta I\% = \frac{I_o - I_s}{I_o} \times 100$$

Where:  $I_0$  is the chemiluminescence intensity of blank

$I_s$  is the chemiluminescence intensity of standard or sample

Gallic acid was selected as a standard antioxidant compound, which was commonly used in the literature to evaluate the TAC of plant-derived foods and beverages because it is a main phenolic antioxidant compound of wine and tea. The TAC of the samples was expressed as gallic acid equivalent (GAE).

**Table 3.2** Experimental sequence for SIA-CL method (SP: syringe pump, SV: selection valve).

Step	Position	Operation
1	SP1 and SP2	Aspirate of H <sub>2</sub> O and luminol as a carrier
2	SV2	Aspirate of H <sub>2</sub> O <sub>2</sub>
3	SV3	Aspirate of sample or standard
4	SV4	Aspirate of K <sub>3</sub> Fe(CN) <sub>6</sub>
5	SV5	Dispense to the flow-cell

### 3.5 DPPH free radical scavenging method

Five gallic acid standard solutions of 0.01 to 0.3 mmol L<sup>-1</sup> were prepared for constructing a calibration curve. 100  $\mu$ L of gallic acid standard solutions or sample were mixed with 3.90 mL of a  $6.0 \times 10^{-5}$  mol L<sup>-1</sup> of DPPH solution and stand for 30 minutes at room temperature before measuring the absorbance at wavelength 515 nm with a fiber optic spectrophotometer (AvaSpec-2048, Avantes Inc., USA). The

scavenging activity of antioxidants was calculated and expressed as % absorbance suppression or antioxidant activity ( $\Delta A\%$ ) according to the formula:

$$\Delta A\% = \frac{A_0 - A_s}{A_0} \times 100$$

Where:  $A_0$  is the absorbance of blank

$A_s$  is the absorbance of standard or sample

### 3.6 Analytical performance

#### 3.6.1 Linearity, LOD and LOQ

The linear range for determination of TAC in beverage samples was investigated. The response of signal with different gallic acid concentrations were measured five times for each standard solution. The calibration graph of  $\Delta I\%$  vs gallic acid concentration was constructed and then, a linear regression equation and correlation coefficient ( $R^2$ ) were obtained.

Limit of detection (LOD) is the lowest concentration of analyte in a sample, which can be reliably detected. Limit of quantitation (LOQ) is the lowest concentration of analyte in a sample, which can be quantitatively determined with accuracy and precision. The LOD and LOQ were calculated from:

$$\text{LOD} = 3S_a/b$$

$$\text{LOQ} = 3S_a/b$$

Where:  $S_a$  is the standard deviation of the intercept

$b$  is the slope of the calibration curve

### 3.6.2 Precision

Six concentrations of gallic acid for the calibration curve (0.5 to 5.0 mmol L<sup>-1</sup>) were used to determine the within-day repeatability and the between-days reproducibility. For the between-days reproducibility, three calibration curves were constructed for the three different days. The % relative standard deviation (RSD) for five measurements was reported by calculating from:

$$\%RSD = \frac{\text{Standard deviation (SD)}}{\text{Mean}} \times 100$$

### 3.6.3 Trueness

The trueness of the analytical method was determined by recovery assays. Wine and tea samples were spiked with 2.0 mmol L<sup>-1</sup> and 0.5 mmol L<sup>-1</sup> of gallic acid, respectively. The % recovery was calculated according to the formula:

$$\%Recovery = \frac{C_s}{C_u + C_a} \times 100$$

Where:  $C_s$  is the concentration of spiked sample

$C_u$  is the concentration of unspiked sample

$C_a$  is the concentration of added gallic acid

### 3.7 Interference study

Some interference such as ethanol, glucose, fructose and sucrose had been investigated. The various amounts of the studied interference were added to the 1.0 mmol L<sup>-1</sup> of gallic acid standard solution. The acceptable concentration ratio of interfering compounds was considered as non-interfering if the relative error of determination is less than ±5%. The % relative error was calculated according to the formula:

$$\% \text{Relative error} = \frac{X_i - X_c}{X_c} \times 100$$

Where:  $X_i$  is the signal of gallic acid and interference mixing

$X_c$  is the signal of gallic acid

### 3.8 Real sample analysis

The diluted wine and tea samples were analyzed using SIA-CL method as described in Section 3.4.2. For the DPPH method, the samples were analyzed as described in Section 3.5. The TAC in samples was calculated from a linear equation of the calibration curve.

The correlation between SIA-CL method and DPPH method were studied by using the GAE value of samples obtained from two methods. After that, a paired t-test at 95% confidence level was used to determine the statistical difference between the % antioxidant activity of the two methods.

## CHAPTER IV

### RESULTS AND DISCUSSION

#### 4.1 Chemiluminescence characteristics

The chemiluminescence reaction between luminol and  $\text{H}_2\text{O}_2$  with the presence of a  $\text{K}_3\text{Fe}(\text{CN})_6$  in alkaline solution was selected for this study because it is a simple, rapid and well-known reaction. The blue light emission of luminol- $\text{H}_2\text{O}_2$ - $\text{K}_3\text{Fe}(\text{CN})_6$  reaction was observed as shown in Figure 4.1. The addition of  $\text{K}_3\text{Fe}(\text{CN})_6$  catalyst which it is a transition metal complex can increase the chemiluminescence intensity due to the decomposition of  $\text{H}_2\text{O}_2$ . According to the Fenton reaction, the decomposition of  $\text{H}_2\text{O}_2$  generate the superoxide radicals which is highly reactive for the oxidation of luminol.

The advantages of a spiral flow-cell made from acrylic plastic material are low cost, inertness and lightweight. Moreover, an opaque white flow-cell can increase the emission intensity because the light cannot pass through the back face of flow-cell. So, it is not necessary to place a mirror on the back face of flow-cell to reflect light back to the detector.



**Figure 4.1** Chemiluminescence from the reaction of luminol with  $\text{H}_2\text{O}_2$  and  $\text{K}_3\text{Fe}(\text{CN})_6$  in a spiral flow-cell.

## 4.2 Optimization of SIA-CL system

### 4.2.1 Sequence of injection

The aspiration sequence of the sample and reagents were studied. The initial conditions for this experiment were: concentration of luminol ( $C_{\text{luminol}}$ ) =  $3.0 \times 10^{-3} \text{ mol L}^{-1}$  in  $0.1 \text{ mol L}^{-1}$  of NaOH, concentration of catalyst or potassium ferricyanide ( $C_{\text{K}_3\text{Fe}(\text{CN})_6}$ ) =  $3.0 \times 10^{-3} \text{ mol L}^{-1}$ , concentration of hydrogen peroxide ( $C_{\text{H}_2\text{O}_2}$ ) =  $3.0 \times 10^{-3} \text{ mol L}^{-1}$ , volume of sample ( $V_{\text{sample}(\text{blank})}$ ) =  $100 \mu\text{L}$ , volume of potassium ferricyanide ( $V_{\text{K}_3\text{Fe}(\text{CN})_6}$ ) =  $100 \mu\text{L}$ , volume of hydrogen peroxide ( $V_{\text{H}_2\text{O}_2}$ ) =  $100 \mu\text{L}$ , volume of luminol ( $V_{\text{luminol}}$ ) =  $2000 \mu\text{L}$  and flow rate of  $5 \text{ mL min}^{-1}$ . The different aspiration sequence were: sample –  $\text{K}_3\text{Fe}(\text{CN})_6$  –  $\text{H}_2\text{O}_2$  – luminol, sample –  $\text{H}_2\text{O}_2$  –  $\text{K}_3\text{Fe}(\text{CN})_6$  – luminol,  $\text{H}_2\text{O}_2$  – sample –  $\text{K}_3\text{Fe}(\text{CN})_6$  – luminol,  $\text{H}_2\text{O}_2$  –  $\text{K}_3\text{Fe}(\text{CN})_6$  – sample – luminol,  $\text{K}_3\text{Fe}(\text{CN})_6$ – $\text{H}_2\text{O}_2$ –sample–luminol and  $\text{K}_3\text{Fe}(\text{CN})_6$ –sample– $\text{H}_2\text{O}_2$ –luminol. The blank CL signals of different aspiration sequence are shown in Figure 4.2. It was found that the highest blank CL signal was observed for the sequence of  $\text{H}_2\text{O}_2$  – sample –  $\text{K}_3\text{Fe}(\text{CN})_6$  – luminol, which was selected for further experiments.

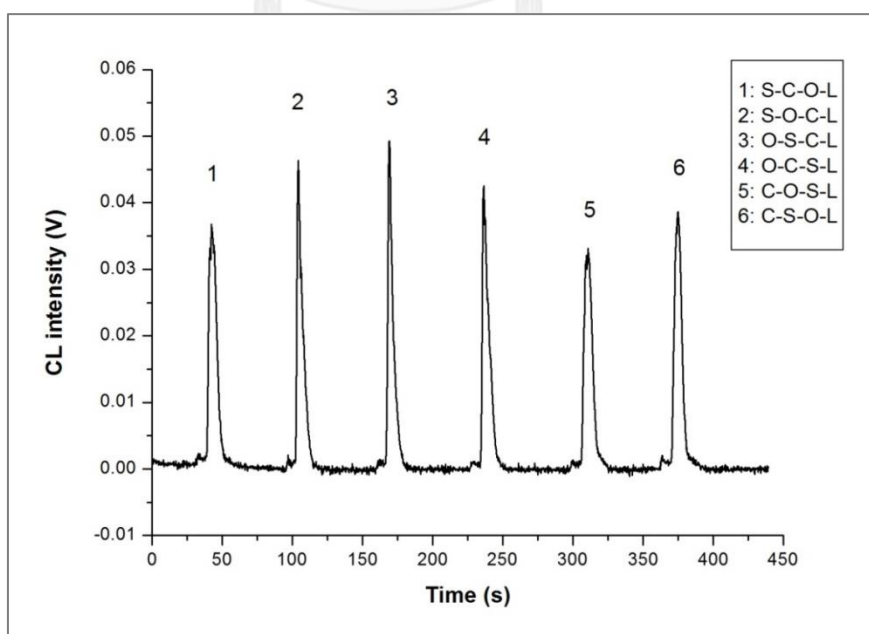


**Figure 4.2** The effect of aspiration sequence on CL intensity. S: sample (blank), C: catalyst ( $\text{K}_3\text{Fe}(\text{CN})_6$ ), O: oxidant ( $\text{H}_2\text{O}_2$ ) and L: luminol.



#### 4.2.2 Effect of sodium hydroxide concentration

The effect of sodium hydroxide concentration was investigated by using the previous conditions. The  $3.0 \times 10^{-3} \text{ mol L}^{-1}$  of luminol in various concentration of sodium hydroxide  $2.0 \times 10^{-2}$  to  $4.0 \times 10^{-1} \text{ mol L}^{-1}$  was studied. The result of the study is shown in Figure 4.3. From the result, it was found that the CL signal increased with increasing the concentration of sodium hydroxide until  $3.0 \times 10^{-1} \text{ mol L}^{-1}$  and became constant. In a strong alkaline condition, luminol solutions are more stable and dissociate more into the dianion form. Therefore, the concentration of sodium hydroxide at  $3.0 \times 10^{-1}$  or  $0.3 \text{ mol L}^{-1}$  was selected as an optimum.

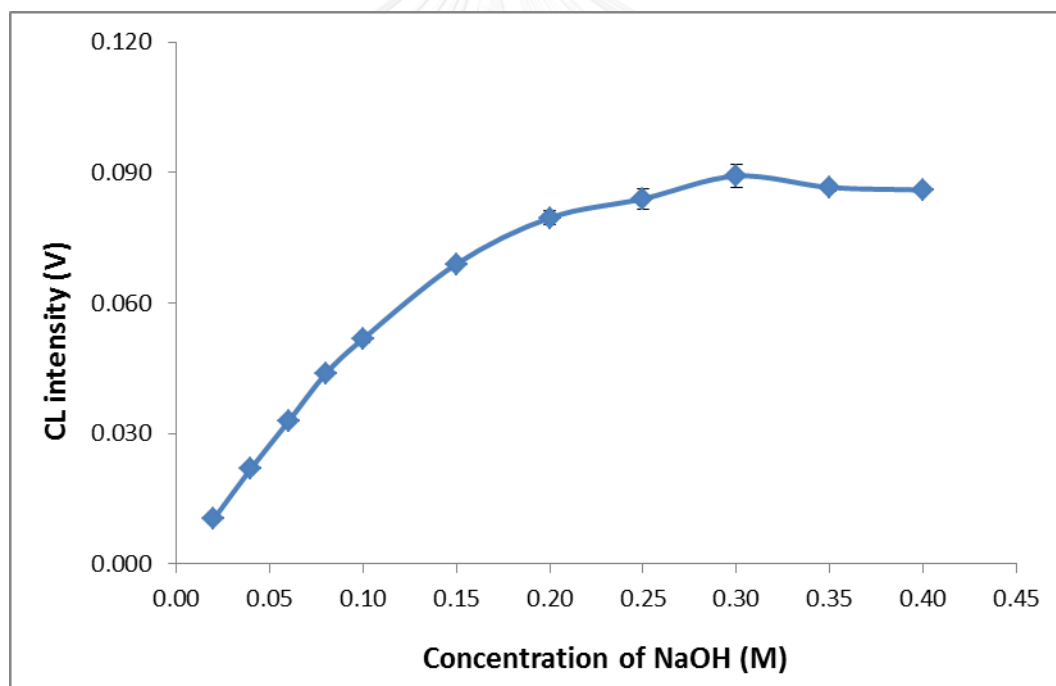


**Figure 4.3** The effect of sodium hydroxide concentration on CL intensity.

### 4.2.3 Effect of luminol concentration

The effect of luminol concentration from  $1.0 \times 10^{-4}$  to  $5.0 \times 10^{-3}$  mol L<sup>-1</sup> in 0.3 mol L<sup>-1</sup> of NaOH was investigated using the following conditions:  $C_{K_3Fe(CN)_6} = 3.0 \times 10^{-3}$  mol L<sup>-1</sup>,  $C_{H_2O_2} = 3.0 \times 10^{-3}$  mol L<sup>-1</sup>,  $V_{\text{sample(blank)}} = 100 \mu\text{L}$ ,  $V_{K_3Fe(CN)_6} = 100 \mu\text{L}$ ,  $V_{H_2O_2} = 100 \mu\text{L}$ ,  $V_{\text{luminol}} = 2000 \mu\text{L}$  and flow rate of  $5 \text{ mL min}^{-1}$ . The effect of luminol concentration on CL intensity was shown in Figure 4.4. The result showed that the CL signal is proportional to the concentration of luminol. The CL intensity increased rapidly when increasing the luminol concentration up to a concentration of  $4.0 \times 10^{-3}$  mol L<sup>-1</sup>. So, to protect the signal variation, the optimum condition of the luminol concentration was chosen to be  $4.0 \times 10^{-3}$  mol L<sup>-1</sup>.

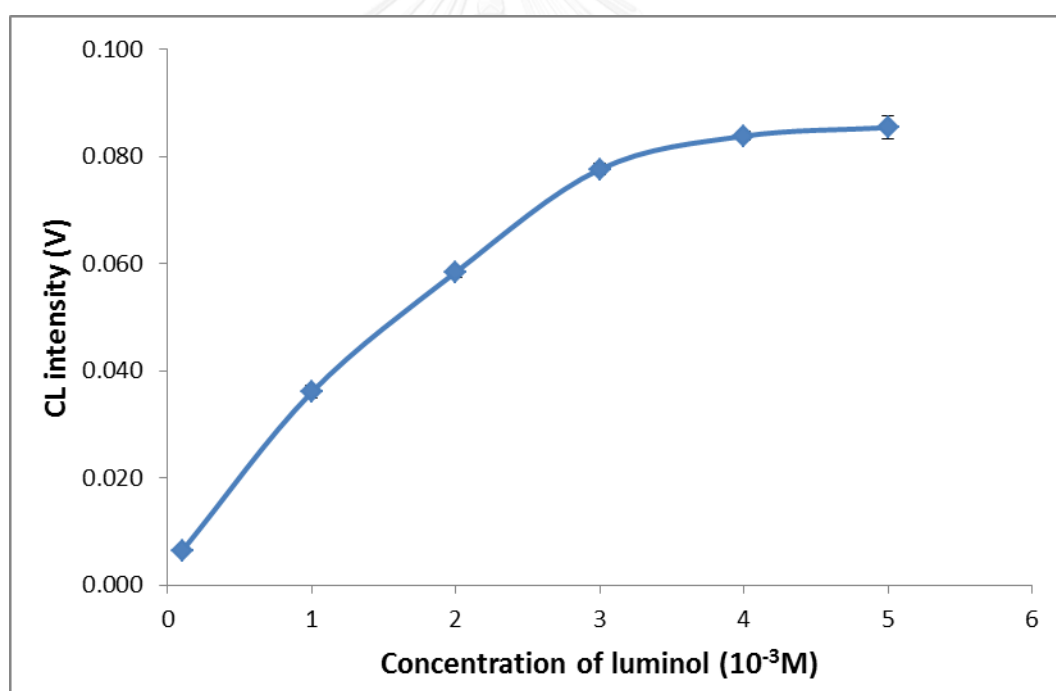


Figure 4.4 The effect of luminol concentration on CL intensity.

#### 4.2.4 Effect of hydrogen peroxide concentration

The effect of hydrogen peroxide concentration in the range of  $3.0 \times 10^{-4} \text{ mol L}^{-1}$  to  $2.0 \times 10^{-2} \text{ mol L}^{-1}$  was studied. The conditions for the study were:  $C_{\text{luminol}} = 4.0 \times 10^{-3} \text{ mol L}^{-1}$ ,  $C_{\text{NaOH}} = 0.3 \text{ mol L}^{-1}$ ,  $C_{\text{K}_3\text{Fe}(\text{CN})_6} = 3.0 \times 10^{-3} \text{ mol L}^{-1}$ ,  $V_{\text{sample}(\text{blank})} = 100 \text{ }\mu\text{L}$ ,  $V_{\text{K}_3\text{Fe}(\text{CN})_6} = 100 \text{ }\mu\text{L}$ ,  $V_{\text{H}_2\text{O}_2} = 100 \text{ }\mu\text{L}$ ,  $V_{\text{luminol}} = 2000 \text{ }\mu\text{L}$  and flow rate of  $5 \text{ mL min}^{-1}$ . It was found that the CL signal increased with increasing the hydrogen peroxide concentration up to  $3.0 \times 10^{-3} \text{ mol L}^{-1}$  and became constant as shown in Figure 4.5. Therefore, the hydrogen peroxide concentration of  $3.0 \times 10^{-3} \text{ mol L}^{-1}$  was chosen as an optimum, which exhibited the highest CL intensity.

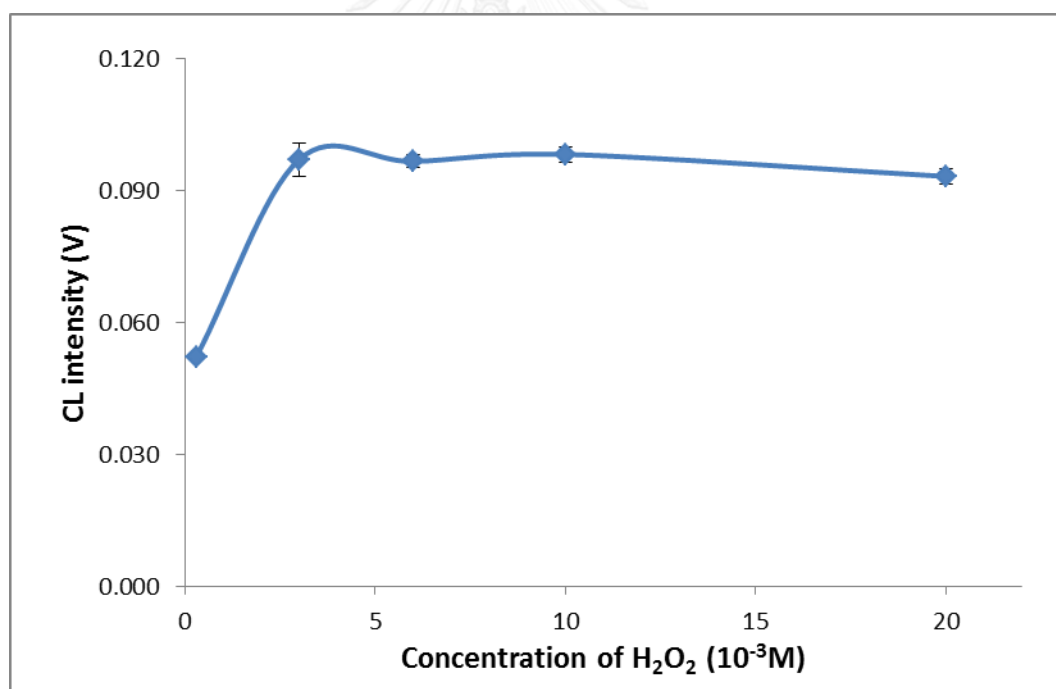


Figure 4.5 The effect of hydrogen peroxide concentration on CL intensity.

#### 4.2.5 Effect of potassium ferricyanide concentration

In this work, the potassium ferricyanide or  $\text{K}_3\text{Fe}(\text{CN})_6$  was used as catalyst for increasing the rate of a reaction. The potassium ferricyanide concentration range of  $1.0 \times 10^{-3}$  to  $4.0 \times 10^{-1} \text{ mol L}^{-1}$  was investigated under these conditions:  $C_{\text{luminol}} = 4.0 \times 10^{-3} \text{ mol L}^{-1}$ ,  $C_{\text{NaOH}} = 0.3 \text{ mol L}^{-1}$ ,  $C_{\text{H}_2\text{O}_2} = 3.0 \times 10^{-3} \text{ mol L}^{-1}$ ,  $V_{\text{sample(blank)}} = 100 \mu\text{L}$ ,  $V_{\text{K}_3\text{Fe}(\text{CN})_6} = 100 \mu\text{L}$ ,  $V_{\text{H}_2\text{O}_2} = 100 \mu\text{L}$ ,  $V_{\text{luminol}} = 2000 \mu\text{L}$  and flow rate of  $5 \text{ mL min}^{-1}$ . The result of the potassium ferricyanide concentration study is shown in Figure 4.6. The CL signal increased with the increasing potassium ferricyanide concentration. However, further increases of catalyst concentration caused a decrease in CL signal. This is because when the reaction occurs very fast, the emission light also disappears quickly. From the result, the maximum CL intensity was observed at  $2.0 \times 10^{-1} \text{ mol L}^{-1}$  of potassium ferricyanide concentration. Therefore, the solution of  $2.0 \times 10^{-1}$  or  $0.2 \text{ mol L}^{-1}$  potassium ferricyanide was selected for further study.

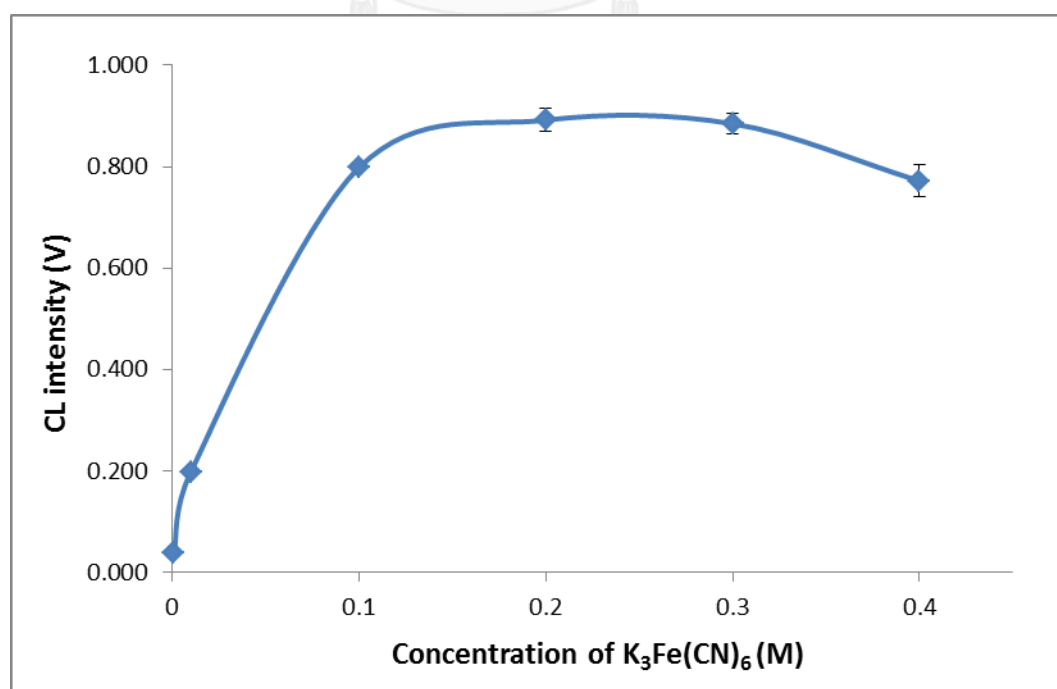
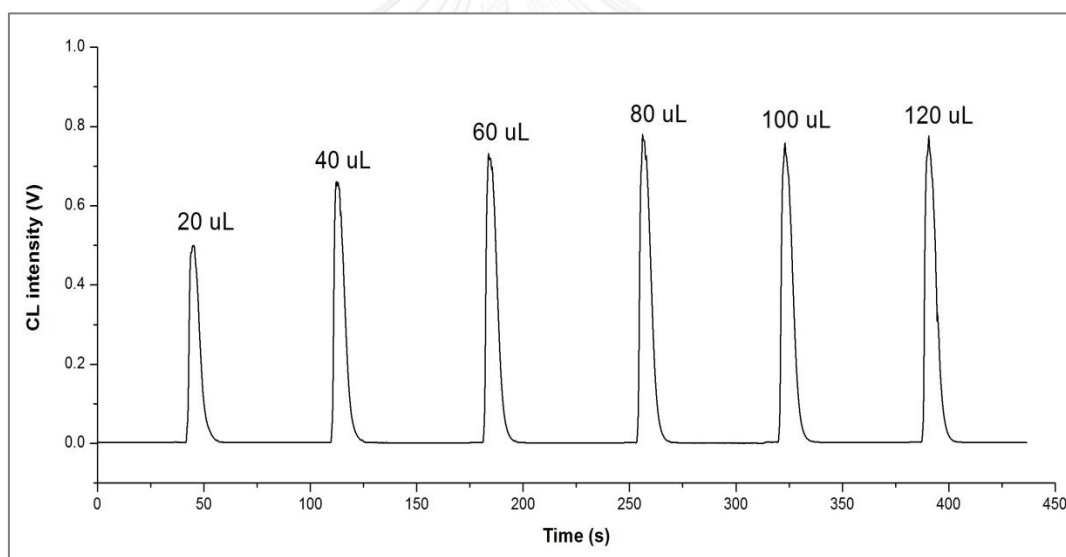


Figure 4.6 The effect of potassium ferricyanide concentration on CL intensity.

#### 4.2.6 The volume of hydrogen peroxide

The volume of hydrogen peroxide was studied in a range of 20 to 120  $\mu\text{L}$ . Using the previous conditions:  $C_{\text{luminol}} = 4.0 \times 10^{-3} \text{ mol L}^{-1}$ ,  $C_{\text{NaOH}} = 0.3 \text{ mol L}^{-1}$ ,  $C_{\text{H}_2\text{O}_2} = 3.0 \times 10^{-3} \text{ mol L}^{-1}$ ,  $C_{\text{K}_3\text{Fe}(\text{CN})_6} = 0.2 \text{ mol L}^{-1}$ ,  $V_{\text{sample}(\text{blank})} = 40 \mu\text{L}$ ,  $V_{\text{K}_3\text{Fe}(\text{CN})_6} = 40 \mu\text{L}$ ,  $V_{\text{luminol}} = 2000 \mu\text{L}$  and flow rate of  $5 \text{ mL min}^{-1}$ . The results are illustrated in Figure 4.7 and Figure 4.8. The CL intensity increased when increasing of hydrogen peroxide volume. The volume of hydrogen peroxide at 80  $\mu\text{L}$  presented the highest and sharp signal. However, excess volume of hydrogen peroxide at 100 and 120  $\mu\text{L}$  provided the same CL signal. Therefore, to minimize the waste product, the volume of hydrogen peroxide at 80  $\mu\text{L}$  was selected as the optimum condition.



**Figure 4.7** SIA-grams recorded from various volumes of hydrogen peroxide.

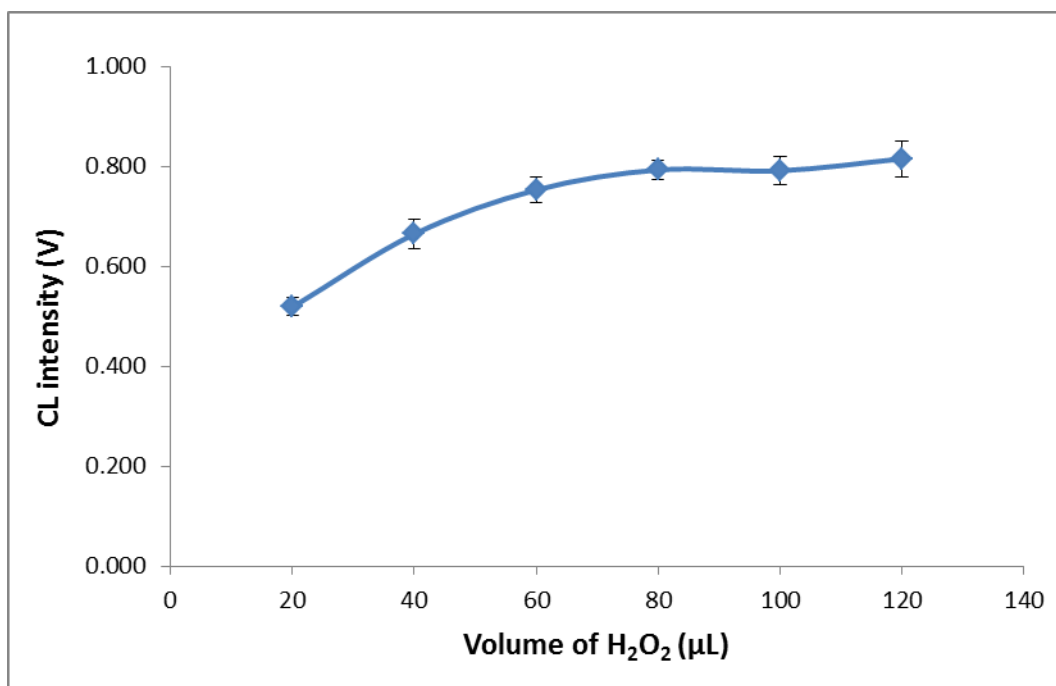


**Figure 4.8** The effect of hydrogen peroxide volume on CL intensity.

#### 4.2.7 The volume of potassium ferricyanide

The potassium ferricyanide volume from 20 to 120 µL was investigated using above conditions:  $C_{\text{luminol}} = 4.0 \times 10^{-3} \text{ mol L}^{-1}$ ,  $C_{\text{NaOH}} = 0.3 \text{ mol L}^{-1}$ ,  $C_{\text{H}_2\text{O}_2} = 3.0 \times 10^{-3} \text{ mol L}^{-1}$ ,  $C_{\text{K}_3\text{Fe}(\text{CN})_6} = 0.2 \text{ mol L}^{-1}$ ,  $V_{\text{sample(blank)}} = 40 \text{ µL}$ ,  $V_{\text{H}_2\text{O}_2} = 80 \text{ µL}$ ,  $V_{\text{luminol}} = 2000 \text{ µL}$  and flow rate of  $5 \text{ mL min}^{-1}$ . The results showed that at higher volume of potassium ferricyanide, the CL intensity increased, but a poor peak shape is also presented at high volume of potassium ferricyanide as can be seen in Figure 4.9 and Figure 4.10. Therefore, the potassium ferricyanide volume of 60 µL was chosen as an optimum because it provides good peak shape and high CL intensity.

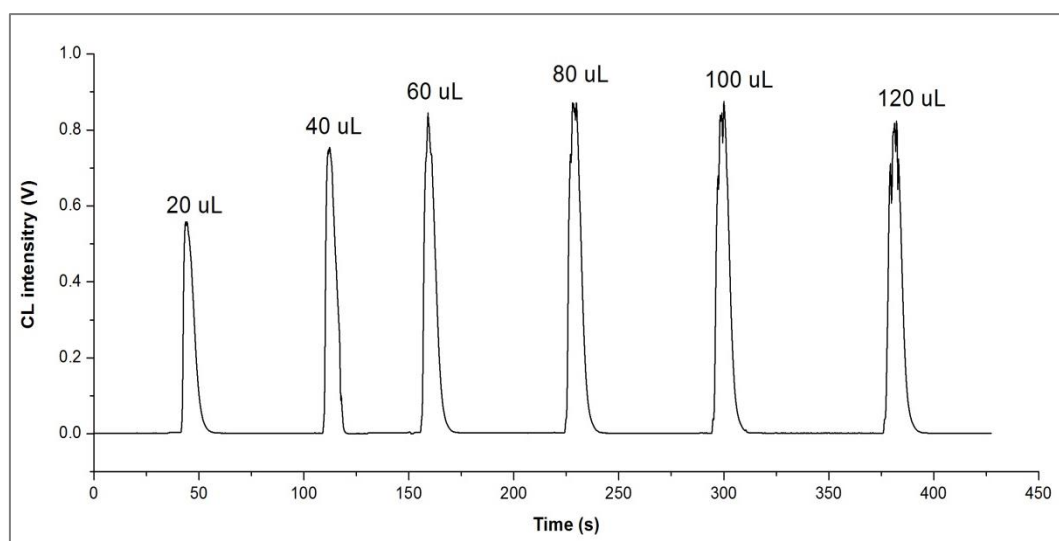


Figure 4.9 SIA-grams recorded from various volumes of potassium ferricyanide.

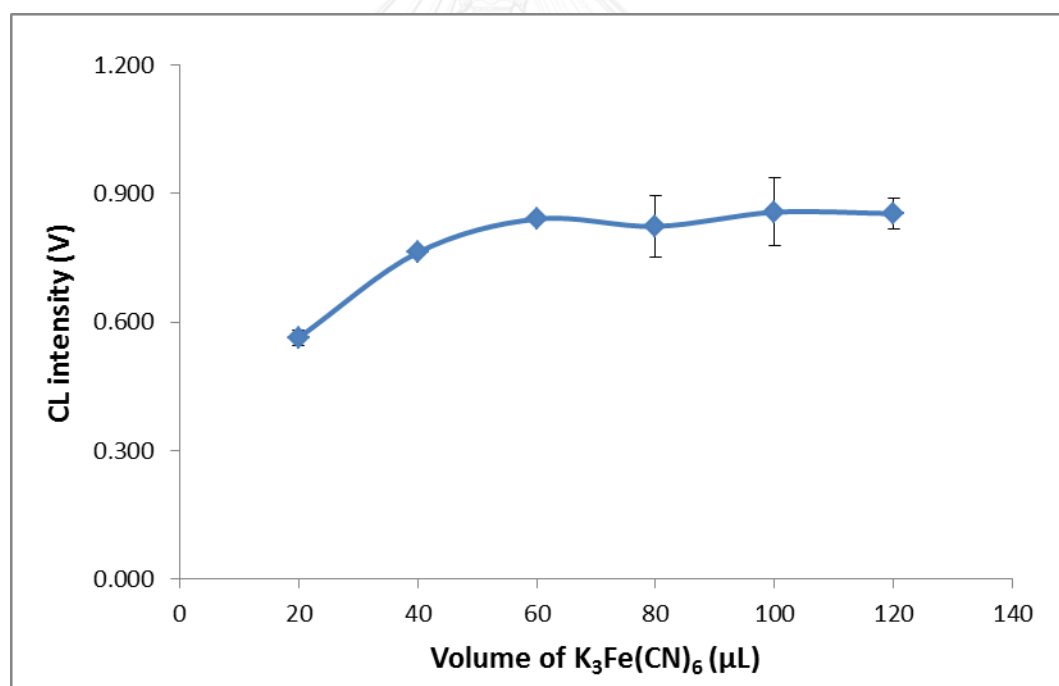
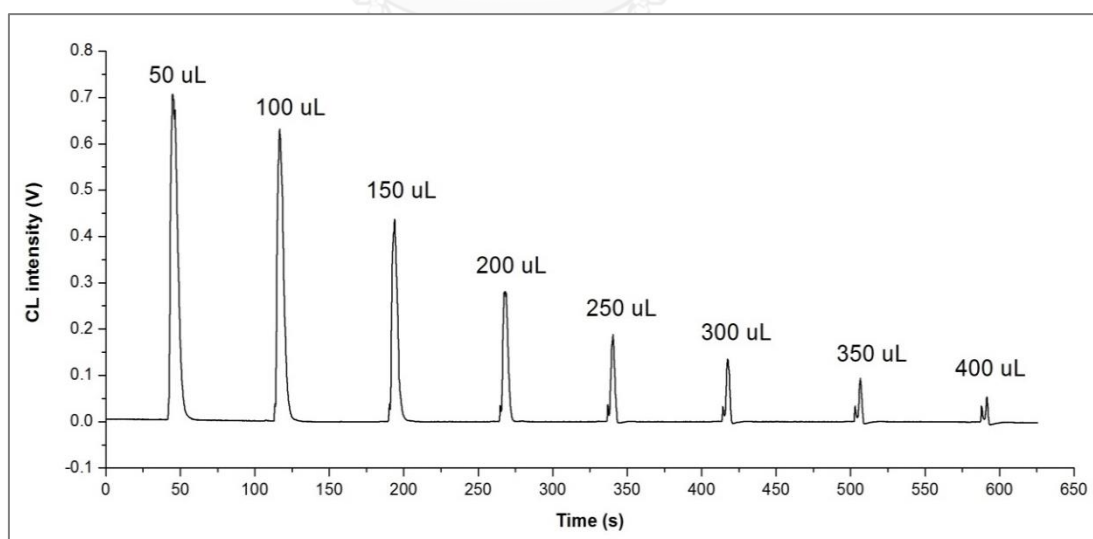


Figure 4.10 The effect of potassium ferricyanide volume on CL intensity.

#### 4.2.8 The volume of sample and standard solution

The effect of the injection volume of  $5.0 \times 10^{-3} \text{ mol L}^{-1}$  gallic acid standard was studied. Under the following conditions:  $C_{\text{luminol}} = 4.0 \times 10^{-3} \text{ mol L}^{-1}$ ,  $C_{\text{NaOH}} = 0.3 \text{ mol L}^{-1}$ ,  $C_{\text{H}_2\text{O}_2} = 3.0 \times 10^{-3} \text{ mol L}^{-1}$ ,  $C_{\text{K}_3\text{Fe}(\text{CN})_6} = 0.2 \text{ mol L}^{-1}$ ,  $V_{\text{H}_2\text{O}_2} = 80 \text{ }\mu\text{L}$ ,  $V_{\text{K}_3\text{Fe}(\text{CN})_6} = 60 \text{ }\mu\text{L}$ ,  $V_{\text{luminol}} = 2000 \text{ }\mu\text{L}$  and flow rate of  $5 \text{ mL min}^{-1}$ . The various volume of gallic acid from 20 to 120  $\mu\text{L}$  was investigated. It was found that the CL intensity decreased rapidly when increasing the volume of gallic acid because with increasing amount of gallic acid, the antioxidant capacity increase, resulting in a decrease in the CL intensity. At higher volume of gallic acid, peak splitting or doublet peak occurred as shown in Figure 4.11. It may be caused by the incomplete mixing of reagent and sample zone. Therefore, the optimum volume of sample and standard at 250  $\mu\text{L}$  was selected. Moreover, the effect of gallic acid volume on signal suppression or antioxidant activity ( $\Delta I\%$ ) was studied. The result showed that the  $\Delta I\%$  is directly proportional to the volumes of gallic acid. The  $\Delta I\%$  continued to increase with increasing volumes of gallic acid as shown in Figure 4.12.



**Figure 4.11** SIA-grams recorded from various volumes of gallic acid.



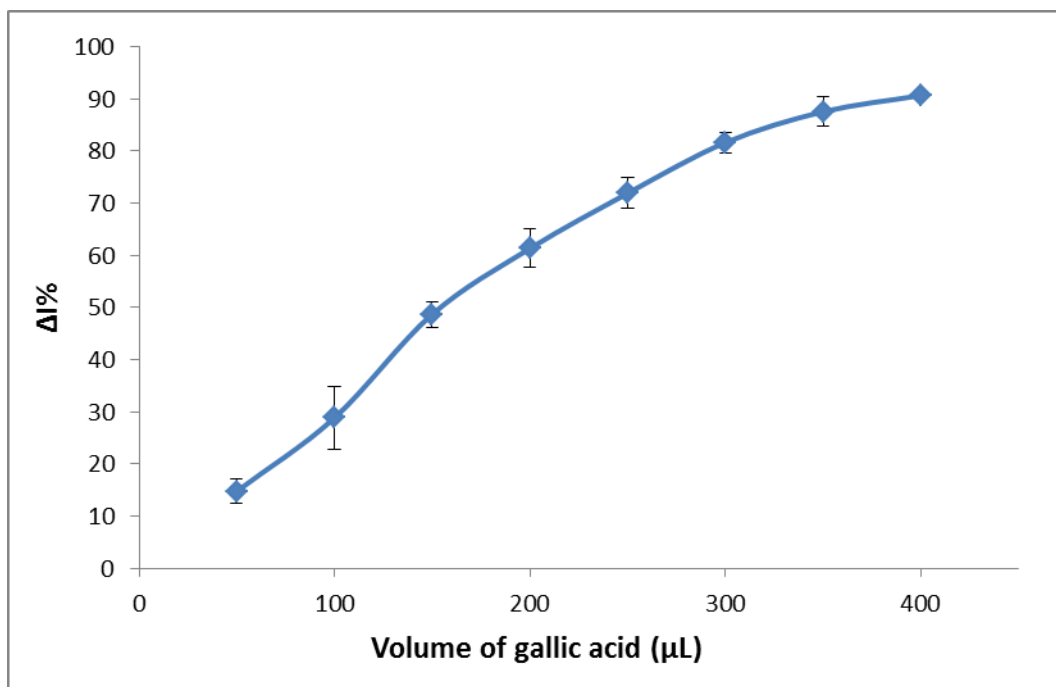


**Figure 4.12** The effect of gallic acid volume on signal suppression.

#### 4.2.9 The volume of luminol

In this work, luminol solution was used as the CL reagent and carrier. Thus, the volume of luminol should be optimal. The volume of luminol in a range of 1000 to 3000 µL was investigated using the previous conditions:  $C_{\text{luminol}} = 4.0 \times 10^{-3} \text{ mol L}^{-1}$ ,  $C_{\text{NaOH}} = 0.3 \text{ mol L}^{-1}$ ,  $C_{\text{H}_2\text{O}_2} = 3.0 \times 10^{-3} \text{ mol L}^{-1}$ ,  $C_{\text{K}_3\text{Fe}(\text{CN})_6} = 0.2 \text{ mol L}^{-1}$ ,  $V_{\text{sample}(\text{blank})} = 250 \text{ µL}$ ,  $V_{\text{H}_2\text{O}_2} = 80 \text{ µL}$ ,  $V_{\text{K}_3\text{Fe}(\text{CN})_6} = 60 \text{ µL}$  and flow rate of  $5 \text{ mL min}^{-1}$ . The effect of luminol volume on CL intensity is shown in Figure 4.13. It was found that when the volume of luminol used lower than 2000 µL some reagent and sample solutions still remain in the tubing because abnormal peaks were observed as shown in Figure 4.13A and 4.13B. Therefore, the optimum volume of luminol at 2000 µL was selected for further experiments.

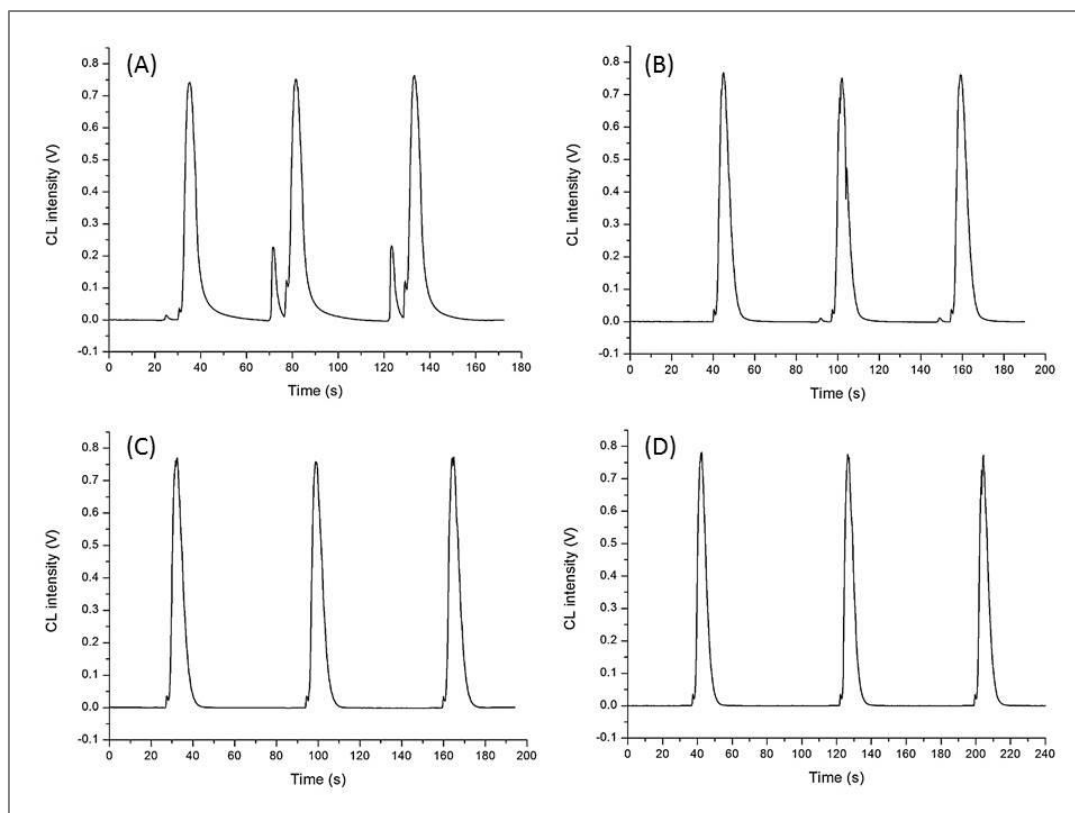


**Figure 4.13** The effect of luminol volume on CL intensity: (A) 1000  $\mu\text{L}$  of luminol, (B) 1500  $\mu\text{L}$  of luminol, (C) 2000  $\mu\text{L}$  of luminol, (D) 2500  $\mu\text{L}$  of luminol.

#### 4.2.10 Effect of detection flow rate

The flow rate for dispensing the solution to the detector from 3.0 to 5.0  $\text{mL min}^{-1}$  was studied. The conditions used were:  $C_{\text{luminol}} = 4.0 \times 10^{-3} \text{ mol L}^{-1}$ ,  $C_{\text{NaOH}} = 0.3 \text{ mol L}^{-1}$ ,  $C_{\text{H}_2\text{O}_2} = 3.0 \times 10^{-3} \text{ mol L}^{-1}$ ,  $C_{\text{K}_3\text{Fe}(\text{CN})_6} = 0.2 \text{ mol L}^{-1}$ ,  $V_{\text{sample}(\text{blank})} = 250 \mu\text{L}$ ,  $V_{\text{H}_2\text{O}_2} = 80 \mu\text{L}$ ,  $V_{\text{K}_3\text{Fe}(\text{CN})_6} = 60 \mu\text{L}$  and  $V_{\text{luminol}} = 2000 \mu\text{L}$ . The effect of detection flow rate on CL intensity is shown in Figure 4.14. From the result, the CL signal increased when increasing the flow rate because of higher flow rate would cause more turbulent flow, resulting in better mixing efficiency. Therefore, the maximum flow rate of a syringe pump at 5.0  $\text{mL min}^{-1}$  was selected as the optimum.

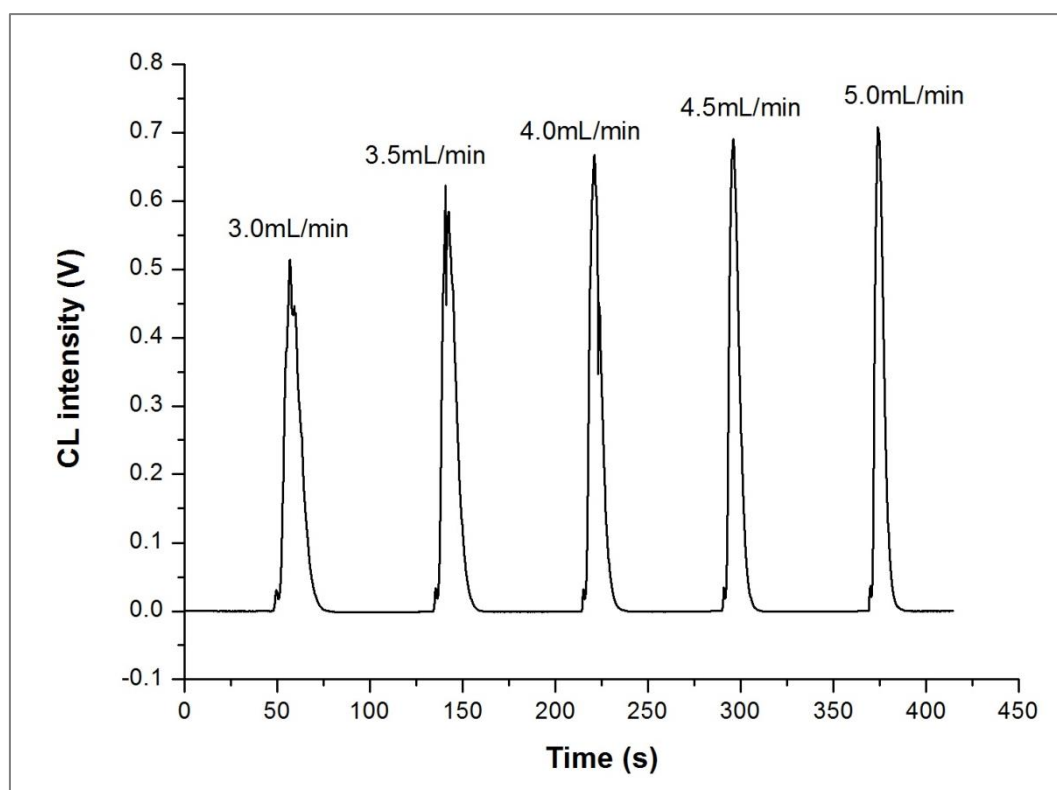


**Figure 4.14** The effect of detection flow rate on CL intensity.

#### 4.2.11 Summary of the optimum conditions for the SIA-CL method

The optimum conditions for SIA-CL method are summarized in Table 4.1. The selected conditions based on these criteria: high CL signal of blank to improve the working range, high value of signal suppression ( $\Delta I\%$ ) to increase the sensitivity, high precision, low reagent consumption and short analysis time to increase the sample throughput.

**Table 4.1** The optimum conditions for the SIA-CL method (S: sample, O: oxidant or  $H_2O_2$ , L: luminol, C: catalyst or  $K_3Fe(CN)_6$ ).

Parameter	Range studied	Selected value
Sequence of injection	S-C-O-L, S-O-C-L, O-S-C-L O-C-S-L, C-O-S-L, C-S-O-L	O-S-C-L
$C_{\text{luminol}}$ ( $\text{mol L}^{-1}$ )	$1.0 \times 10^{-4} - 5.0 \times 10^{-3}$	$4.0 \times 10^{-3}$
$C_{\text{NaOH}}$ ( $\text{mol L}^{-1}$ )	$2.0 \times 10^{-2} - 4.0 \times 10^{-1}$	$3.0 \times 10^{-1}$
$C_{H_2O_2}$ ( $\text{mol L}^{-1}$ )	$3.0 \times 10^{-4} - 2.0 \times 10^{-2}$	$3.0 \times 10^{-3}$
$C_{K_3Fe(CN)_6}$ ( $\text{mol L}^{-1}$ )	$1.0 \times 10^{-3} - 4.0 \times 10^{-1}$	$2.0 \times 10^{-1}$
$V_{H_2O_2}$ ( $\mu\text{L}$ )	20 – 120	80
$V_{K_3Fe(CN)_6}$ ( $\mu\text{L}$ )	20 – 120	60
$V_{\text{sample/std.}}$ ( $\mu\text{L}$ )	50 – 400	250
$V_{\text{luminol/carrier}}$ ( $\mu\text{L}$ )	1000 – 3000	2000
Flow rate ( $\text{mL min}^{-1}$ )	3.0 – 5.0	5.0

### 4.3 Analytical performance

#### 4.3.1 Linearity, LOD and LOQ

Under optimum conditions, the CL signal of different gallic acid concentrations were measured five times for each standard solution by SIA-CL method. The example of SIA-grams of blank solution and antioxidant standard solution is shown in Figure 4.15. The CL intensity was converted to the %signal suppression ( $\Delta I\%$ ). Then, a calibration graph plotted between the  $\Delta I\%$  and gallic acid concentration (GAE,  $\text{mmol L}^{-1}$ ) was constructed. The  $\Delta I\%$  was increased linearly proportional to the gallic acid concentrations as shown in Figure 4.16. The linear range was obtained in the range of 0.5 to 5.0  $\text{mmol L}^{-1}$  with the regression equation:  $y = 12.035X + 3.2111$ ,  $R^2 = 0.9969$ . The limit of detection (LOD) and quantitation (LOQ) were calculated as 0.25 and 0.84  $\text{mmol L}^{-1}$ , respectively. The proposed method has a very fast analysis time with the sample throughput of 60 samples  $\text{h}^{-1}$ .

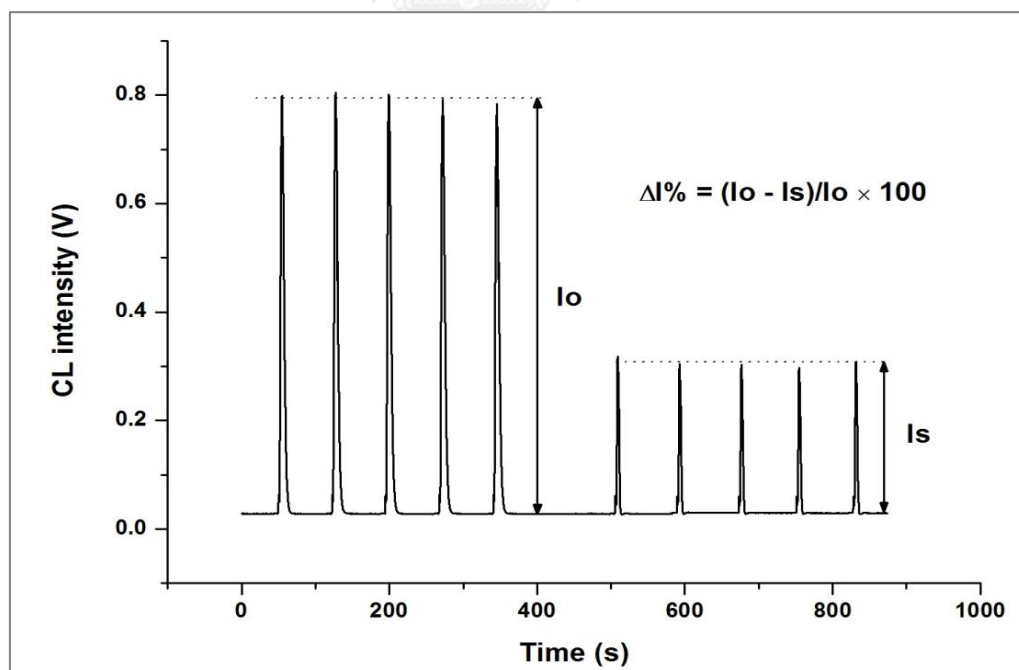


**Figure 4.15** SIA-grams of blank solution ( $I_o$ ) and antioxidant solution ( $I_s$ ),  
 $C_{\text{gallic acid}} = 4.0 \text{ mmol L}^{-1}$ .

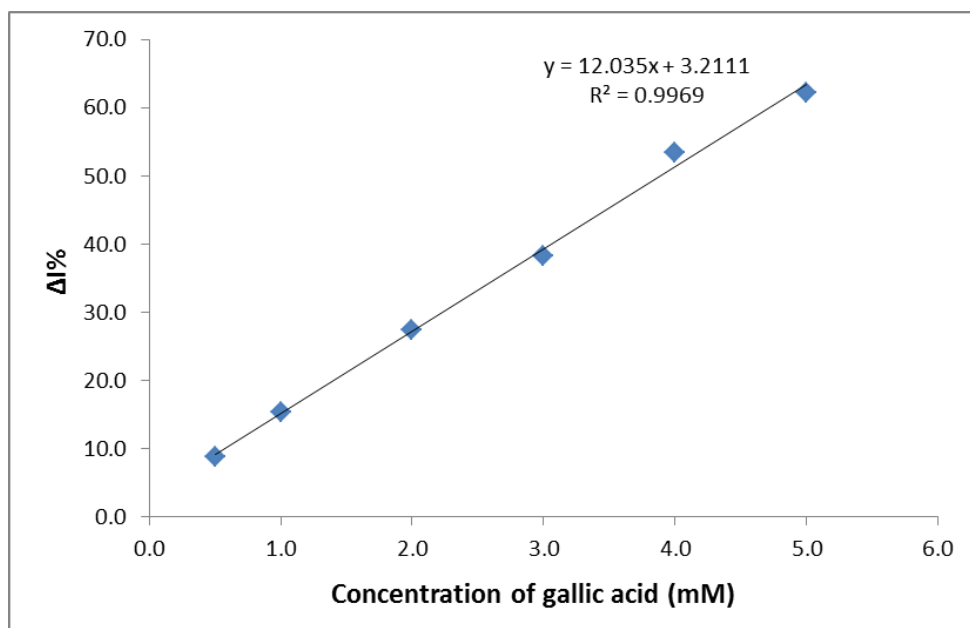
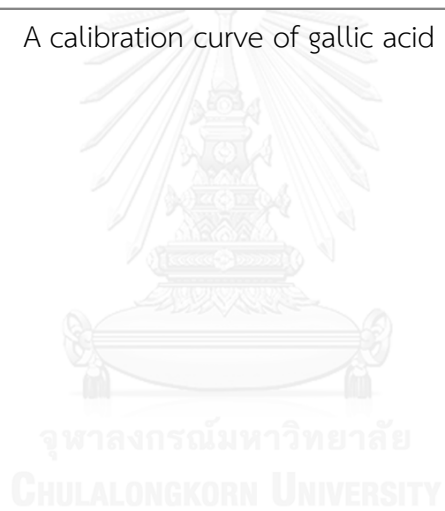


**Figure 4.16** A calibration curve of gallic acid using SIA-CL method.



### 4.3.2 Precision

The within-day repeatability of the developed SIA-CL method was expressed as a relative standard deviation (RSD) of five replicates of six gallic acid standard solutions in concentration range from 0.5 to 5.0 mmol L<sup>-1</sup>. The %RSD of within-day repeatability was obtained in the range of 0.5 to 1.4% (Table 4.2). For the between-days reproducibility, the six concentration levels of gallic acid were measured five times and the calibration plots were constructed for the three different days ( $n \times k = 5 \times 3 = 15$  total replicates). The %RSD of between-days reproducibility was obtained to be in the range of 2.2 to 5.4% (Table 4.2). The results showed that the %RSD values of within-day repeatability and between-days reproducibility were satisfactory. Thus, the developed SIA-CL method has high precision.

**Table 4.2** The within-day repeatability and between-days reproducibility of the SIA-CL method.

Conc. of Gallic acid (mmol L <sup>-1</sup> )	0.5	1.0	2.0	3.0	4.0	5.0
<b>%RSD within-day repeatability (n=5)</b>						
	1.1	0.6	0.5	0.9	1.0	1.4
<b>%RSD between-days reproducibility (n × k = 5 × 3 = 15)</b>						
	5.4	2.2	2.2	2.4	3.2	2.6

### 4.3.3 Trueness

For the recovery experiments, three samples of wine and tea before and after spiking with 2.0 and 0.5 mmol L<sup>-1</sup> of gallic acid were analyzed. The results are shown in Table 4.3. The recoveries of wine and tea samples were in the range of 95.8 to 105.6%. These values were considered acceptable according to the AOAC guidelines, demonstrating that the method has high accuracy and reliability.

**Table 4.3** Recovery study of gallic acid in wine and tea samples.

No. of Sample	Type of sample	Gallic acid (mmol L <sup>-1</sup> )		Recovery (%)
		Unspiked	Spiked	
<b>Wine samples</b>				
1	red wine	1.20	3.34	104.4
2	white wine	0.76	2.83	102.3
3	rose wine	1.70	3.91	105.6
<b>Tea samples</b>				
4	green tea	2.31	2.69	95.8
5	oolong tea	2.95	3.32	96.1
6	black tea	2.37	2.89	100.8



#### 4.4 Interference study

Some substances that can cause interferences for determination of the TAC in wine are ethanol and glucose. In tea, the interfering substances such as glucose, fructose and sucrose were studied. The responses of 1.0 mmol L<sup>-1</sup> of gallic acid with the various amount of the studied interference were determined. A substance was considered as non-interfering if the relative error of determination less than  $\pm 5\%$ . The maximum concentration of each interfering compound which causes no interference is listed in Table 4.4. The results showed that the proposed method presents good selectivity. However, the interference can be avoided with high dilution of the sample solution before analysis.

**Table 4.4** The acceptable concentration of interfering compounds in the determination of gallic acid by SIA-CL method.

Interferences	Concentration (mM)	Relative error (%)
Ethanol	1500	-0.41
Glucose	500	-3.93
Fructose	200	-3.59
Sucrose	200	-0.09

#### 4.5 Real sample analysis

The developed SIA-CL method was applied to the determination of the TAC in wine and tea samples. The samples were diluted with deionized water as described in Section 3.2. The results were expressed as GAE values which was calculated from the calibration curve of gallic acid (using the regression equation:  $y = 12.035X + 3.2111$ ). The TAC in beverage samples obtained from developed SIA-CL method and DPPH method were compared as shown in Table 4.5. From the results, the GAE values obtained from two methods were absolutely different. Generally, the determination of TAC by different *in vitro* methods can produce different absolute values because it is different in the terms of reaction mechanisms and experimental conditions [42-44]. However, a good correlation between SIA-CL method and DPPH method was observed. The correlation coefficient ( $R^2$ ) for wine and tea samples was 0.9989 and 0.9997, respectively. These results showed that the present method could be used for ranking of samples according to their TAC [18, 20].

**Table 4.5** Total antioxidant content in wine and tea samples obtained by the SIA-CL and DPPH method.

No. of Sample	Type of sample	% Antioxidant activity*		GAE (mmol L <sup>-1</sup> )	
		SIA-CL	DPPH	SIA-CL	DPPH
<b>Wine samples</b>					
1	red wine	27.6	39.5	20.3	2.61
2	white wine	24.5	15.4	3.54	0.22
3	rose wine	29.9	27.4	4.44	0.44
<b>Tea samples</b>					
4	green tea	28.3	33.5	4.17	1.09
5	oolong tea	30.9	38.1	4.59	1.26
6	black tea	17.0	15.9	1.15	0.09

\* % Antioxidant activity or  $\Delta I\%$  was calculated from diluted samples as described in Section 3.2.

Additionally, the GAE values of wine and tea samples obtained by the proposed method and published literature were studied as shown in Table 4.6. The GAE values were reported as milligram of gallic acid equivalents per litre of sample. From the data, it was found that the results are in agreement with previous literature. The differences in total antioxidant content between the proposed method and published literature result from different types of wines and teas, depending on location and production process.

**Table 4.6** The GAE values of wine and tea samples obtained by the proposed method and published literature.

Literature	GAE (mg L <sup>-1</sup> )					
	Red wine	White wine	Rose wine	Green tea	oolong tea	Black tea
This study	3451	602	755	709	780	196
Porgali et al. [45] (Turkish wines)	1837-3467	-	-	-	-	-
Buyuktuncel et al. [46] (Turkish wines)	2600-4847	-	-	-	-	-
Lugemwa et al. [47] (South African wines)	2434-2703	-	-	-	-	-
Carruba et al. [48, 49] (Italian wines)	-	179-542	-	-	-	-
Gattuso et al. [50] (Italian wines)	-	672	-	-	-	-
Gigliotti et al. [51] (Italian wines)	-	-	440	-	-	-
Owczarek et al. [52] (Indian teas)	-	-	-	1314	-	939
L. Fu et al. [53] (Chinese teas)	-	-	-	235	- 867	

Moreover, a paired t-test at 95% confidence level was used to compare the % antioxidant activity between the developed method and the standard method as DPPPH method. It was found that the values of  $t_{\text{stat}}$  (-0.62) <  $t_{\text{critical}}$  (2.57). Therefore, there was no significant difference between the two methods. The results of paired t-test are shown in Figure 4.17. These results confirmed that the developed SIA-CL method has high accuracy and reliability for determination of the TAC.

t-Test: Paired Two Sample for Means		
	<i>SIA-CL</i>	<i>DPPH</i>
Mean	26.36666667	28.3
Variance	25.90266667	113.9
Observations	6	6
Pearson Correlation	0.756082964	
Hypothesized Mean Difference	0	
df	5	
t Stat	-0.623619863	
P(T<=t) one-tail	0.280109968	
t Critical one-tail	2.015048373	
P(T<=t) two-tail	0.560219935	
t Critical two-tail	2.570581836	

**Figure 4.17** Paired t-test comparison of % antioxidant activity between SIA-CL method and DPPH method.

## CHAPTER V

### CONCLUSIONS

In this research, the sequential injection analysis (SIA) with chemiluminescence (CL) system was developed for the determination of total antioxidant content (TAC) in wines and beverages. The method is based on the inhibition effect of antioxidants on luminol-H<sub>2</sub>O<sub>2</sub>-K<sub>3</sub>Fe(CN)<sub>6</sub> chemiluminescence reaction in alkaline condition. The developed SIA-CL method is rapid (with a sample throughput of 60 samples h<sup>-1</sup>), automated, uncomplicated and consumes less chemical. Moreover, the home-made chemiluminescence detection system was fabricated from inexpensive materials and a small size light-to-voltage optical sensor was used as an alternative detector. The developed SIA-CL method was successfully applied for the determination of TAC in plant-derived beverages (wine and tea samples). The working range for gallic acid used to express the TAC was obtained from 0.5 to 5.0 mmol L<sup>-1</sup> with a good detection limit of 0.25 mmol L<sup>-1</sup> and quantitation limit of 0.84 mmol L<sup>-1</sup>. Additionally, the proposed method offers high precision (with the %RSD of between-days reproducibility of 2.2 to 5.4%). A comparison of the results between the SIA-CL method and DPPH method for the analysis of wine and tea samples provided a good correlation and there was no significant difference between two methods, demonstrating that the proposed method is accurate and reliable for measurement of TAC in plant-derived beverage samples. Therefore, the developed SIA-CL method could be used as a routine method for the analysis and the quality control of beverage products.

## REFERENCES

- [1] Pokorny, J., Yanishlieva, N., and Gordon, M. Antioxidant in food-practical applications. North America: Woodhead Publishing Limited, 2001.
- [2] Cadenas, E. and Packer, L. Handbook of antioxidants, ed. 2nd. New York: Marcel Dekker, Inc, 2002.
- [3] Nalewajko-Sieliwoniuk, E., Tarasewicz, I., and Kojlo, A. Flow injection chemiluminescence determination of the total phenolics levels in plant-derived beverages using soluble manganese(IV). Analytical Chimica Acta 668(1) (2010): 19-25.
- [4] Stevenson, D.E. and Hurst, R.D. Polyphenolic phytochemicals-just antioxidants or much more? Cellular and Molecular Life Sciences 64(22) (2007): 2900-16.
- [5] Vauzour, D., Rodriguez-Mateos, A., Corona, G., Oruna-Concha, M.J., and Spencer, J.P. Polyphenols and human health: prevention of disease and mechanisms of action. Nutrients 2(11) (2010): 1106-31.
- [6] Carmona-Jimenez, Y., Garcia-Moreno, M.V., Igartuburu, J.M., and Garcia Barroso, C. Simplification of the DPPH assay for estimating the antioxidant activity of wine and wine by-products. Food Chemistry 165 (2014): 198-204.
- [7] Pérez-Jiménez, J., et al. Updated methodology to determine antioxidant capacity in plant foods, oils and beverages: extraction, measurement and expression of results. Food Research International 41(3) (2008): 274-285.
- [8] Seeram, N.P., et al. Comparison of antioxidant potency of commonly consumed polyphenol-rich beverages in the united states. Journal of Agricultural and Food Chemistry 56 (2008): 1415-1422.
- [9] Villano, D., Fernandez-Pachon, M.S., Troncoso, A.M., and Garcia-Parrilla, M.C. The antioxidant activity of wines determined by the ABTS<sup>•+</sup> method: influence of sample dilution and time. Talanta 64(2) (2004): 501-9.
- [10] Zhang, Y., et al. Evaluation of antioxidant activity of ten compounds in different tea samples by means of an on-line HPLC-DPPH assay. Food Research International 53(2) (2013): 847-856.

- [11] Borges, G., Degeneve, A., Mullen, W., and Crozier, A. Identification of flavonoid and phenolic antioxidants in black currants, blueberries, raspberries, red currants, and cranberries. Journal of Agricultural and Food Chemistry 58(7) (2010): 3901-9.
- [12] Barroso, M.F., et al. DNA-based biosensor for the electrocatalytic determination of antioxidant capacity in beverages. Biosensors and Bioelectronics 26(5) (2011): 2396-401.
- [13] Wang, X., Jiao, C., and Yu, Z. Electrochemical biosensor for assessment of the total antioxidant capacity of orange juice beverage based on the immobilizing DNA on a poly l-glutamic acid doped silver hybridized membrane. Sensors and Actuators B: Chemical 192 (2014): 628-633.
- [14] Piljac-Žegarac, J., Valek, L., Stipčević, T., and Martinez, S. Electrochemical determination of antioxidant capacity of fruit tea infusions. Food Chemistry 121(3) (2010): 820-825.
- [15] Arnao, M.B. Some methodological problems in the determination of antioxidant activity using chromogen radicals: a practical case. Trends in Food Science & Technology 11(11) (2000): 419-421.
- [16] Garcia-Campana, A.M. and Baeyens, W.R.G.E. Chemiluminescence in analytical chemistry. New York: Marcel Dekker, Inc, 2001.
- [17] Christodouleas, D., Fotakis, C., Economou, A., Papadopoulos, K., Timotheou-Potamia, M., and Calokerinos, A. Flow-based methods with chemiluminescence detection for food and environmental analysis: a review. Analytical Letters 44(1-3) (2011): 176-215.
- [18] Fassoula, E., Economou, A., and Calokerinos, A. Development and validation of a sequential-injection method with chemiluminescence detection for the high throughput assay of the total antioxidant capacity of wines. Talanta 85(3) (2011): 1412-8.
- [19] Giokas, D.L., Vlessidis, A.G., and Evmiridis, N.P. On-line selective detection of antioxidants free-radical scavenging activity based on Co(II)/EDTA-induced luminol chemiluminescence by flow injection analysis. Analytica Chimica Acta 589(1) (2007): 59-65.

- [20] Karampelas, D., Economou, A., and Calokerinos, A. A novel hybrid flow-injection/sequential-injection methodology for the rapid evaluation of the total antioxidant capacity of wines using inhibition of the alkaline luminol-potassium permanganate chemiluminescent reaction. Microchemical Journal 118 (2015): 223-230.
- [21] Marquele, F.D., Di Mambro, V.M., Georgetti, S.R., Casagrande, R., Valim, Y.M.L., and Fonseca, M.J.V. Assessment of the antioxidant activities of Brazilian extracts of propolis alone and in topical pharmaceutical formulations. Journal of Pharmaceutical and Biomedical Analysis 39(3-4) (2005): 455-462.
- [22] Nalewajko-Sieliwoniuk, E., Nazaruk, J., Antypiuk, E., and Kojło, A. Determination of phenolic compounds and their antioxidant activity in *Erigeron acris* L. extracts and pharmaceutical formulation by flow injection analysis with inhibited chemiluminescent detection. Journal of Pharmaceutical and Biomedical Analysis 48(3) (2008): 579-586.
- [23] Pires, C.K., Marques, K.L., Santos, J.L.M., Lapa, R.A.S., Lima, J.L.F.C., and Zagatto, E.A.G. Chemiluminometric determination of carvedilol in a multi-pumping flow system. Talanta 68(2) (2005): 239-244.
- [24] Christodouleas, D., Fotakis, C., Papadopoulos, K., Yannakopoulou, E., and Calokerinos, A.C. Development and validation of a chemiluminogenic method for the evaluation of antioxidant activity of hydrophilic and hydrophobic antioxidants. Analytica Chimica Acta 652(1-2) (2009): 295-302.
- [25] Costin, J.W., Barnett, N.W., Lewis, S.W., and McGillivray, D.J. Monitoring the total phenolic/antioxidant levels in wine using flow injection analysis with acidic potassium permanganate chemiluminescence detection. Analytica Chimica Acta 499(1-2) (2003): 47-56.
- [26] Francis, P.S., Costin, J.W., Conlan, X.A., Bellomarino, S.A., Barnett, J.A., and Barnett, N.W. A rapid antioxidant assay based on acidic potassium permanganate chemiluminescence. Food Chemistry 122(3) (2010): 926-929.
- [27] Christodouleas, D.C., Giokas, D.L., Garyfali, V., Papadopoulos, K., and Calokerinos, A.C. An automatic FIA-CL method for the determination of



- antioxidant activity of edible oils based on peroxyoxalate chemiluminescence. Microchemical Journal 118 (2015): 73-79.
- [28] Mansouri, A., Makris, D.P., and Kefalas, P. Determination of hydrogen peroxide scavenging activity of cinnamic and benzoic acids employing a highly sensitive peroxyoxalate chemiluminescence-based assay: structure–activity relationships. Journal of Pharmaceutical and Biomedical Analysis 39(1–2) (2005): 22-26.
- [29] Lei, R., et al. Enhanced anodic  $\text{Ru}(\text{bpy})_3^{2+}$  electrogenerated chemiluminescence by polyphenols. Analytica Chimica Acta 625(1) (2008): 13-21.
- [30] Kim, W. Phenol removal from saturated porous media using horseradish peroxidase mediated oxidative polymerization process. Civil Engineering Kansas State University, 2007.
- [31] Jirum, J. and Srihanam, P. Oxidants and antioxidants: sources and mechanism. Academic Journal Rajabhat Kalasin University 1(1) (2011): 59-70.
- [32] Preedy, V. Processing and impact on antioxidants in beverages. New York: Elsevier Inc., 2014.
- [33] Podemska, K., Orzeł, A., Podsiadły, R., and Sokółowska, J. Chemiluminescence – mystery of cold light. Chemik International 67(11) (2013): 1085-1096.
- [34] Flow-based analysis for environmental monitoring [Online]. Available from: <http://www.globalfia.com/downloads/no3.pdf> [2017, May 2]
- [35] Sequential injection analysis [Online]. Available from: [http://www.flowinjection.com/images/Sequential\\_Injection.pdf](http://www.flowinjection.com/images/Sequential_Injection.pdf) [2017, May 2]
- [36] Murillo Pulgarín, J.A., García Bermejo, L.F., and Carrasquero Durán, A. Use of the attenuation of luminol-perborate chemiluminescence with flow injection analysis for the total antioxidant activity in tea infusions, wines, and grape seeds. Food Analytical Methods 5(3) (2011): 366-372.
- [37] Araujo, A.R., Maya, F., Saraiva, M.L., Lima, J.L., Estela, J.M., and Cerda, V. Flow system for the automatic screening of the effect of phenolic compounds on the luminol-hydrogen peroxide-peroxidase chemiluminescence system. Luminescence 26(6) (2011): 571-8.

- [38] Jain, V.K. Effect of catalyst on luminol - hydrogen peroxide-water chemiluminescence system. Asian Journal of Pharmaceutical Analysis 3(4) (2013): 134-140.
- [39] Alapont, A.G., Zamora, L.L., and Calatayud, J.M.n. Indirect determination of paracetamol in pharmaceutical formulations by inhibition of the system luminol-H<sub>2</sub>O<sub>2</sub>-Fe(CN)<sub>6</sub><sup>3-</sup> chemiluminescence. Journal of Pharmaceutical and Biomedical Analysis 21 (1999): 311-317.
- [40] Mohr, S., et al. Precision milled flow-cells for chemiluminescence detection. Analyst 134(11) (2009): 2233-8.
- [41] Terry, J.M., et al. Chemiluminescence detection flow cells for flow injection analysis and high-performance liquid chromatography. Analytical and Bioanalytical Chemistry 403(8) (2012): 2353-60.
- [42] Ahmad, S., Arshad, M.A., Ijaz, U.K., Rashid, F., and Azam, R. Review on methods used to determine antioxidant activity. International Journal of Multidisciplinary Research and Development 1(1) (2014): 35-40.
- [43] Karadag, A., Ozcelik, B., and Saner, S. Review of methods to determine antioxidant capacities. Food Analytical Methods 2(1) (2009): 41-60.
- [44] Prior, R.L., Wu, X., and Schaich, K. Standardized methods for the determination of antioxidant capacity and phenolics in foods and dietary supplements. Journal of Agricultural and Food Chemistry 53(10) (2005): 4290-302.
- [45] Porgali, E. and Büyüktuncel, E. Determination of phenolic composition and antioxidant capacity of native red wines by high performance liquid chromatography and spectrophotometric methods. Food Research International 45(1) (2012): 145-154.
- [46] Büyüktuncel, E., Porgali, E., and Çolak, C. Comparison of total phenolic content and total antioxidant activity in local red wines determined by spectrophotometric methods. Food and Nutrition Sciences 5 (2014): 1660-1667.

- [47] Lugemwa, F.N., Snyder, A.L., and Shaikh, K. Determination of radical scavenging activity and total phenols of wine and spices: a randomized study. Antioxidants 2(3) (2013): 110-21.
- [48] Carruba, E., Agostino, S., Pastena, B., Alagna, C., and Torina, G. Indagine analytica su vini siciliani monovarietali. I. vini bianchi. Rivista di Viticoltura e di Enologia 34 (1981): 359-400.
- [49] Carruba, E., Agostino, S., Pastena, B., Alagna, C., and Torina, G. Indagine analytica su vini siciliani monovarietali. II. vini rossi. Rivista di Viticoltura e di Enologia 35 (1982): 47-79.
- [50] Gattuso, A.M., Indovina, M.C., and Pirrone, L. Costituenti polifenolici di vini bianchi grezzi della sicilia occidentale. Vignevini 13(4) (1986): 35-38.
- [51] Gigliotti, A. and Bucelli, P. Influenza della tecnologia di vinificazione adottata sulle caratteristiche organolettiche del vino rosato. Rivista di Viticoltura e di Enologia 39 (1986): 158-172.
- [52] Lubomila Owczarek, Jasińska, U., Osińska, M., and Skapska, S. Juices and beverages with a controlled phenolic content and antioxidant capacity. Polish Journal of Food and Nutrition Sciences 13 (2004): 261-268.
- [53] Fu, L., et al. Total phenolic contents and antioxidant capacities of herbal and tea infusions. International Journal of Molecular Sciences 12(4) (2011): 2112-24.



## APPENDIX A

## Chemiluminescence characteristics of luminol

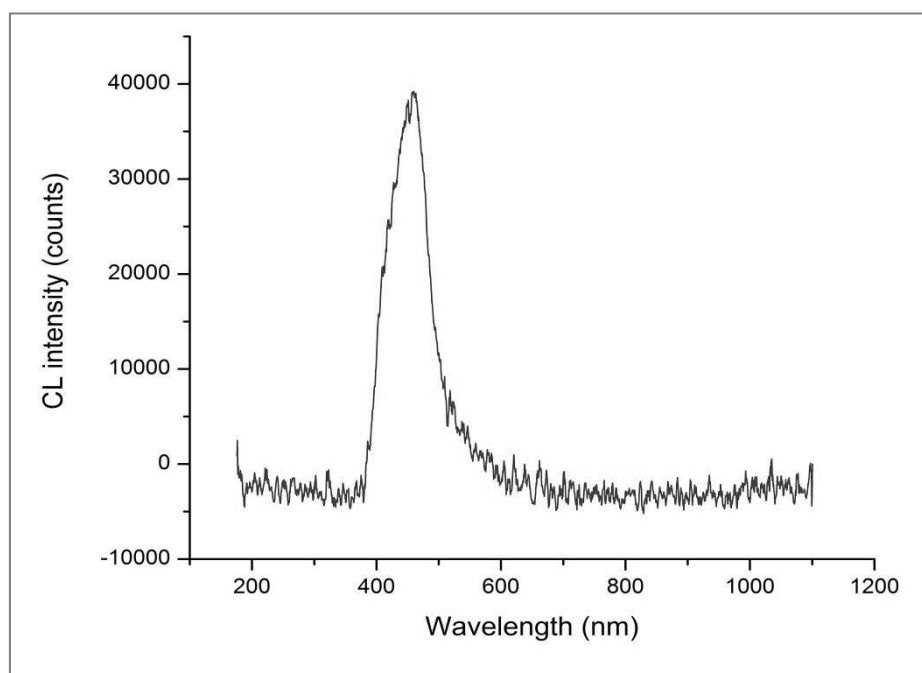


**Figure A1** Chemiluminescence spectrum of luminol with hydrogen peroxide with the presence of potassium ferricyanide catalyst recorded by AvaSpec-2048 fiber-optic spectrophotometer.

## APPENDIX B

## SIA-grams of gallic acid standard

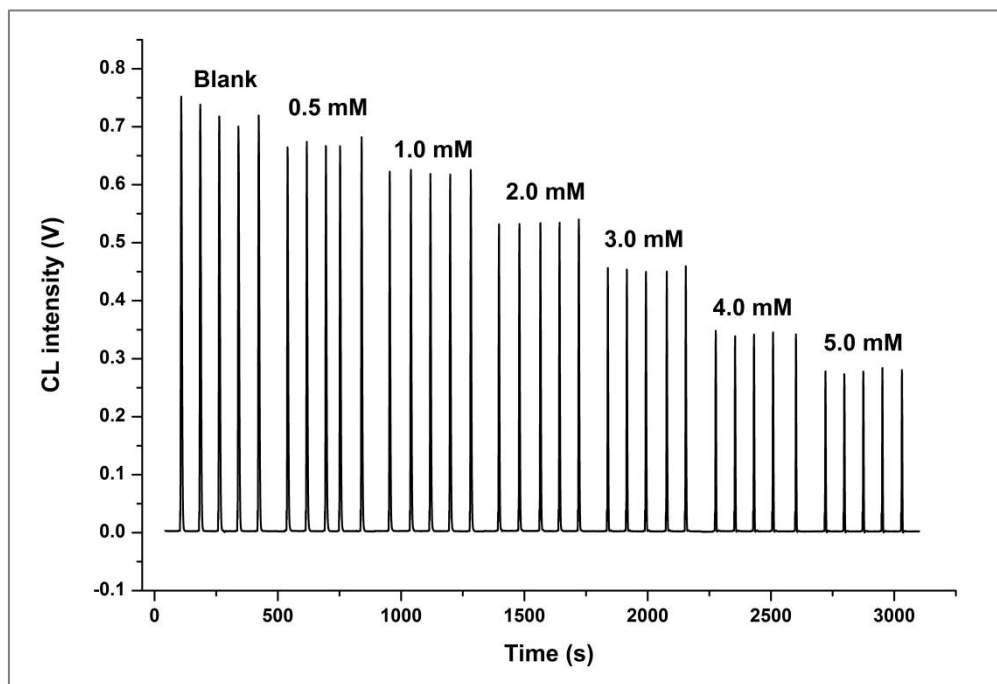


Figure B1 SIA-grams of various gallic acid concentrations using SIA-CL method.

APPENDIX C  
DPPH free radical scavenging method

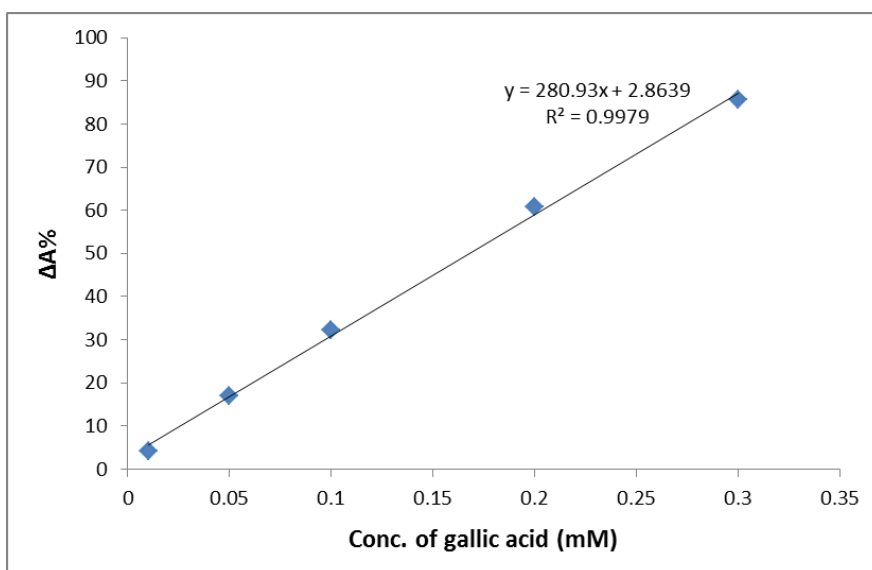
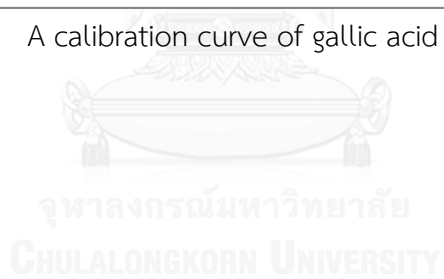


Figure C1 A calibration curve of gallic acid using DPPH method.



## APPENDIX D

## Correlation between SIA-CL method and DPPH method

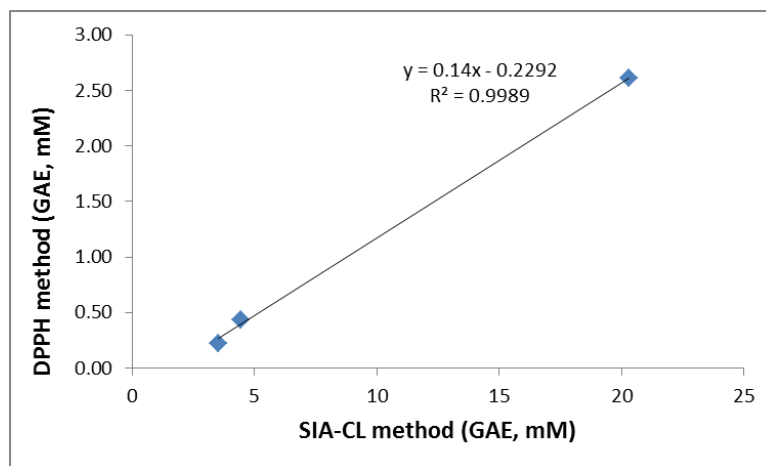


Figure D1 Correlation plot between the SIA-CL method and DPPH method for wine samples (n=3).

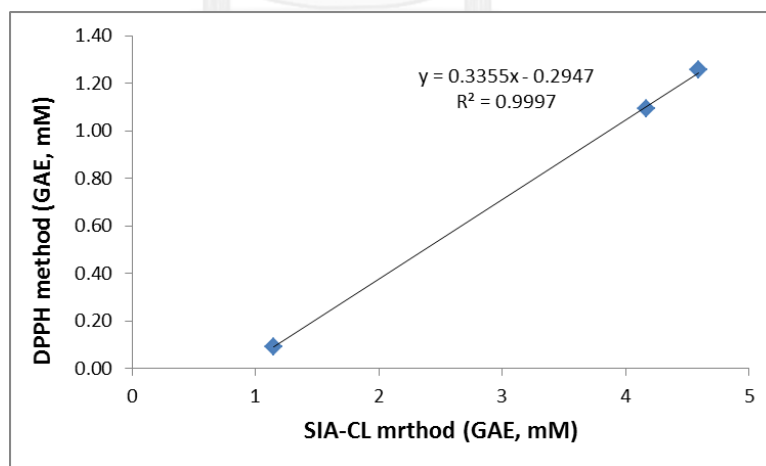


Figure D2 Correlation plot between the SIA-CL method and DPPH method for tea samples (n=3).



## APPENDIX E

## Development of chemiluminescence detector

## Part I: Design of chemiluminescence detector

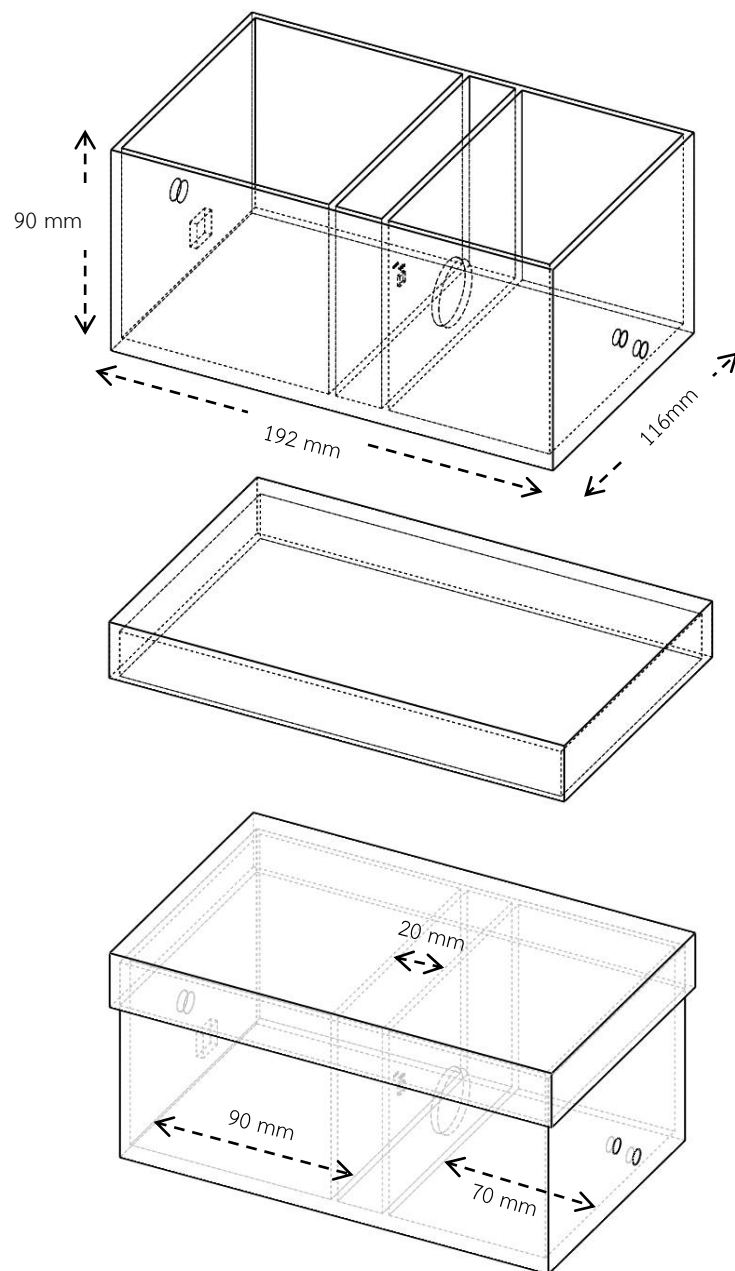


Figure E1 The 3D design of developed chemiluminescence detector.

## Part II: Light-to-voltage optical sensors

Product data sheet from Texas Advanced Optoelectronic Solutions (TAOC)  
Inc. Available from: [www.ams.com](http://www.ams.com)

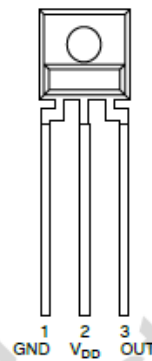


### TSL12S, TSL13S, TSL14S LIGHT-TO-VOLTAGE CONVERTERS

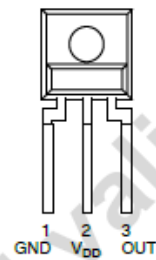
TAOS001E - SEPTEMBER 2007

- Converts Light Intensity to Output Voltage
- Monolithic Silicon IC Containing Photodiode, Transconductance Amplifier, and Feedback Components
- Single-Supply Operation . . . 2.7 V to 5.5 V
- High Irradiance Responsivity . . . Typical 246 mV/( $\mu\text{W}/\text{cm}^2$ ) at  $\lambda_p = 640 \text{ nm}$  (TSL12S)
- Low Supply Current . . . 1.1 mA Typical
- Sidelooker 3-Lead Plastic Package
- RoHS Compliant (-LF Package Only)

PACKAGE S  
SIDELOOKER  
(FRONT VIEW)



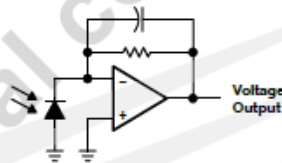
PACKAGE SM  
SURFACE MOUNT  
SIDELOOKER  
(FRONT VIEW)



#### Description

The TSL12S, TSL13S, and TSL14S are cost-optimized, highly integrated light-to-voltage optical sensors, each combining a photodiode and a transimpedance amplifier (feedback resistor = 80 M $\Omega$ , 20 M $\Omega$ , and 5 M $\Omega$ , respectively) on a single monolithic integrated circuit. The photodiode active area is 0.5 mm  $\times$  0.5 mm and the sensors respond to light in the range of 320 nm to 1050 nm. Output voltage is linear with light intensity (irradiance) incident on the sensor over a wide dynamic range. These devices are supplied in a 3-lead clear plastic sidelooker package (S). When supplied in the lead (Pb) free package, the device is RoHS compliant.

#### Functional Block Diagram



## TSL12S, TSL13S, TSL14S LIGHT-TO-VOLTAGE CONVERTERS

TAC0301E - SEPTEMBER 2007

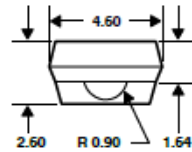
### MECHANICAL DATA

The TSL12S, TSL13S, and TSL14S are supplied in a clear 3-lead through-hole package with a molded lens.

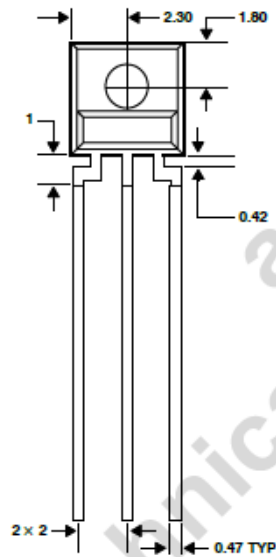
PACKAGE S

PLASTIC SINGLE-IN-LINE SIDE-LOOKER PACKAGE

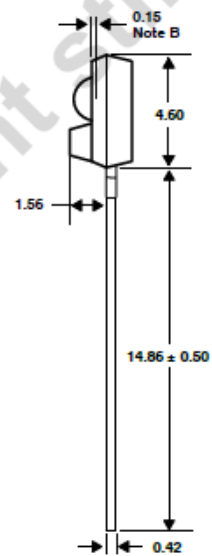
TOP VIEW



FRONT VIEW



SIDE VIEW



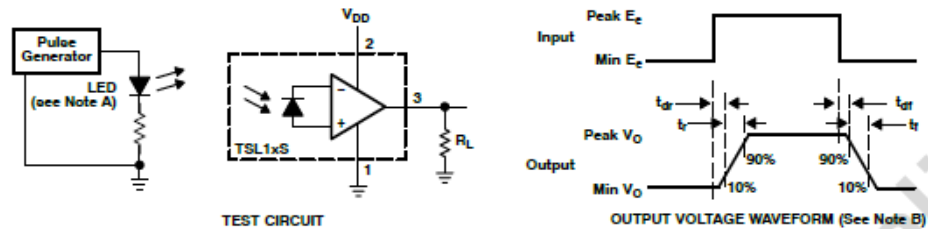
Lead Free  
Available

- NOTES:
- All linear dimensions are in millimeters; tolerance is  $\pm 0.25$  mm unless otherwise stated.
  - Dimension is to center of lens area, which is located below the package face.
  - The  $0.50$  mm  $\times$   $0.50$  mm integrated photodiode active area is typically located in the center of the lens and  $0.97$  mm below the top of the lens surface.
  - Index of refraction of clear plastic is 1.55.
  - Lead finish for TSL1xS: solder dipped, 63% Sn/37% Pb. Lead finish for TSL1xS-LF: solder dipped, 100% Sn.
  - This drawing is subject to change without notice.

## TSL12S, TSL13S, TSL14S LIGHT-TO-VOLTAGE CONVERTERS

TA09051E - SEPTEMBER 2007

### PARAMETER MEASUREMENT INFORMATION



- NOTES: A. The input irradiance is supplied by a pulsed AlInGaP light-emitting diode with the following characteristics:  $\lambda_p = 640 \text{ nm}$ ,  $t_r < 1 \mu\text{s}$ ,  $t_f < 1 \mu\text{s}$ .
- B. The output waveform is monitored on an oscilloscope with the following characteristics:  $t_r < 100 \text{ ns}$ ,  $Z_i \geq 1 \text{ M}\Omega$ ,  $C_i \leq 20 \text{ pF}$ .

Figure 1. Switching Times

### TYPICAL CHARACTERISTICS

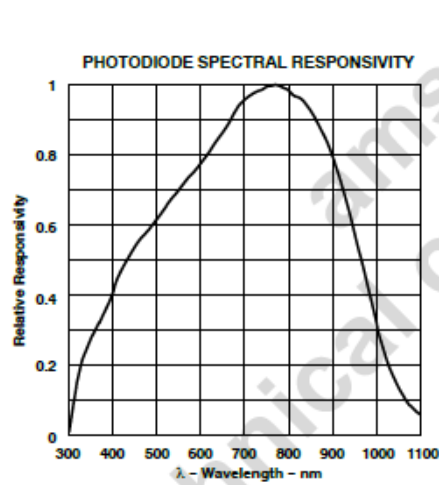


Figure 2

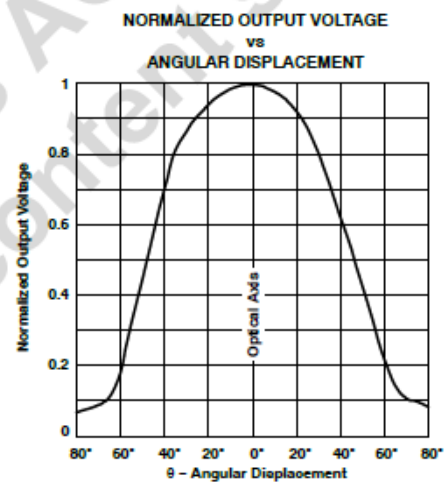


Figure 3

TSL12S, TSL13S, TSL14S  
LIGHT-TO-VOLTAGE CONVERTERS

TAC0501E - SEPTEMBER 2007

TYPICAL CHARACTERISTICS

TSL12S

RISING EDGE DYNAMIC CHARACTERISTICS  
vs.  
PEAK OUTPUT VOLTAGE

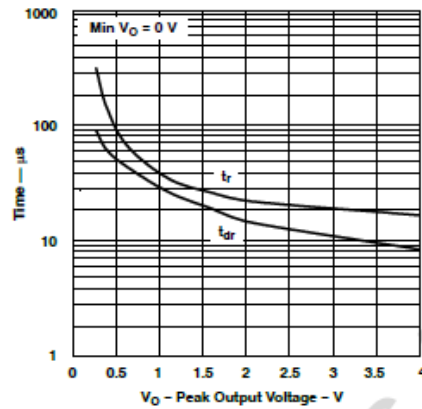


Figure 4

RISING EDGE DYNAMIC CHARACTERISTICS  
vs.  
PEAK OUTPUT VOLTAGE

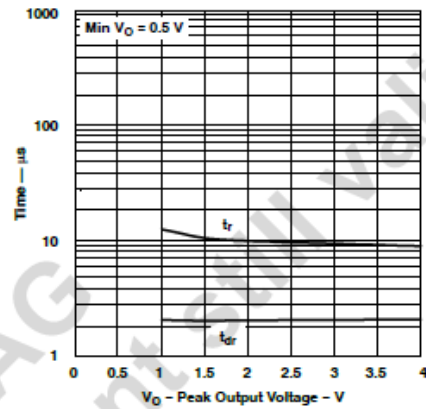


Figure 5

FALLING EDGE DYNAMIC CHARACTERISTICS  
vs.  
PEAK OUTPUT VOLTAGE

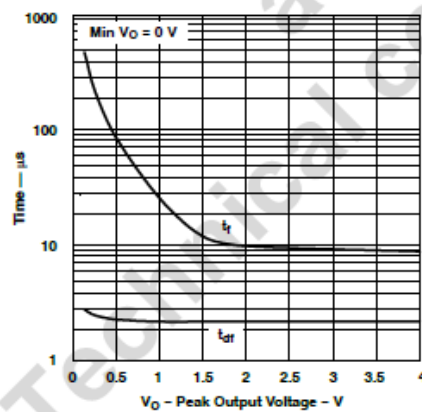


Figure 6

FALLING EDGE DYNAMIC CHARACTERISTICS  
vs.  
PEAK OUTPUT VOLTAGE

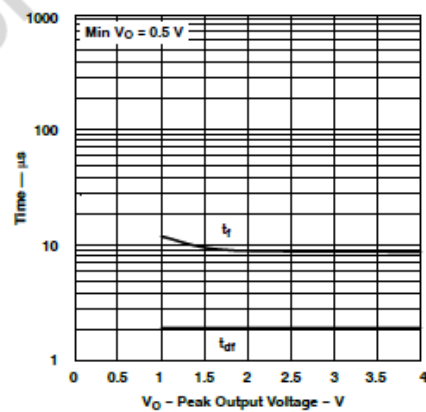


Figure 7

## VITA

Ms. Masinee Saowadee was born on November 13, 1991 in Chiang Rai, Thailand. She graduated with a bachelor's degree of Science in Applied Chemistry from Mea Fah Luang University in 2014. She decided to continue her studies with a master's degree of Science in Chemistry at Chulalongkorn University and will be complete in 2017. Her address after graduation is 3 Moo 2, Patung, Meachan, Chiangrai, Thailand.

Proceeding:

Masinee Saowadee, Passapol Ngamukot “Development of chemiluminescence system for determination of total antioxidant content in beverages” Proceeding of Pure and Applied Chemistry International Conference 2017, Centra Government Complex Hotel & Convention Centre Bangkok, Thailand, February 2-3, 2017, pp 119-123.